Study on Efficient Piezoelectric Energy Harvesting with Frequency Self-tuning

By

Yukun Cheng

A thesis submitted to the Faculty of Graduate Studies of

The University of Manitoba

in partial fulfilment of the requirements of the degree of

MASTER OF SCIENCE

Department of Mechanical Engineering

Faculty of Engineering

University of Manitoba

Winnipeg, Manitoba

Copyright © 2016 by Yukun Cheng

Abstract

A frequency self-tuning energy harvesting methodology is proposed to achieve efficient energy harvesting. To simulate the self-tuning process, a theoretical model of the harvester made of an aluminum beam bonded with piezoelectric patches is developed for numerical simulation. The energy harvesting is realized by converting ambient vibration to electric charge through piezoelectric patches on the host beam. To accomplish the frequency self-tuning process, a control voltage is applied on a piezoelectric stack actuator to tune the natural frequency of the beam harvester matching the major excitation frequency of the ambient vibration with large power generation. Two tuning methods with different electric circuits are developed to find the most efficient and feasible self-tuning process, which is then further verified by the finite element method (FEM). Research findings show that the optimal frequency self-tuning method significantly increases the power output from the harvester by more than 26 times compared with the one without tuning.

Acknowledgements

Foremost, I would like to express my sincere appreciation to my supervisor Dr. Nan Wu for his continuous support of my graduate study and research, for his patience, enthusiasm, and valuable guidance. His supervision definitely provided me with the tools that I needed to choose the right direction and successfully complete my thesis. I could not have imagined having a better advisor and mentor for my M.Sc study.

I would also like to thank my colleagues in our lab: Shengjie Zhao and Buddhi Wimarshana for the great time we worked together.

Last but not the least, I owe my deepest gratitude to my parents for their unconditional love, support and encouragement throughout my life. Thanks for giving me strength to reach for the stars and chase my dreams.

Contents

Contents ..... **iii**

List of Tables ..... **v**

List of Figures ..... **vi**

List of Symbols ..... **vii**

1 Introduction **1**

1.1 Background 1

1.2 Literature review 3

1.2.1 Mechanical tuning methods 6

1.2.2 Electrical tuning methods 7

1.3 Research objectives 10

2 Theoretical model and methodology **11**

2.1 A theoretical model of the beam energy harvester with compressive axial force 12

2.2 Iteration numerical method solving the forced vibration response with continuous frequency-tuning 17

3 Self-tuning with a feedback filtering circuit **23**

3.1 Principle of the feedback filtering circuit 24

3.2 Numerical simulations and discussions 24

3.3 Conclusions 26

4 Self-tuning with a tuning capacitor **33**

4.1 Design of the tuning circuit 34

4.2 Numerical simulations and discussions 36

4.3 Finite element analysis for verification of self-tuning process 40

4.4 Conclusions 43

5 Conclusions and future work 63

List of Tables

Table 3-1 Dimensions and material properties of the piezoelectric coupled beam. 28

Table 4-1 Dimensions and material properties of the energy harvesting system..... 45

Table 4-2 Parameter study with different thickness of piezoelectric patches. 45

Table 4-3 Parameter study with different length of piezoelectric patches. 46

List of Figures

Fig. 2-1 A simply supported beam energy harvester with compressive axial force. 22

Fig. 3-1 Schematic diagram and geometries of proposed energy harvester. 29

Fig. 3-2 Generated voltage and output electric power on piezoelectric patches without self-tuning. 30

Fig. 3-3 Generated voltage and output electric power on piezoelectric patches with self-tuning. 31

Fig. 3-4 RMS value of the output electric power versus different length of piezoelectric patches. 32

Fig. 4-1 Charging of the tuning capacitor through the diode bridge circuit. 47

Fig. 4-2 Design of the proposed self-tuning energy harvesting system. 50

Fig. 4-3 Transverse displacement of the beam harvester with/without tuning. 51

Fig. 4-4 Voltages and power on piezoelectric patches with/without tuning. 53

Fig. 4-5 Convergence study of the RMS power output with different iteration step lengths. 54

Fig. 4-6 RMS value of the output power versus different thickness of piezoelectric patches. 55

Fig. 4-7 Generated charge, voltage and power versus different length of piezoelectric patches. 56

Fig. 4-8 RMS value of output electric power versus different capacitance and resistance of the tuning circuit. 57

Fig. 4-9 Finite element model of the host beam bonded with piezoelectric patches. 58

Fig. 4-10 Transverse displacement of beam harvester (a) without tuning (b) with tuning. 60

Fig. 4-11 Voltage generation from FEM analysis. 61

Fig. 4-12 Convergence study of different element size. 62

List of Symbols

L : Length of simply supported beam

a : Length of piezoelectric patches

L_1&L_2 : Distance from the left end of the host beam to piezoelectric patches

b : Width of the host beam and piezoelectric patches

h : Thickness of the host beam

h_1 : Thickness of piezoelectric patches

h_2 : Thickness of one layer of the piezoelectric stack actuator

A_1 : Cross section area of the piezoelectric stack actuator

E : Young's modulus of the host beam

E_p : Young's modulus of the piezoelectric patch

ρ : Mass density of the host beam

ρ' : Mass density of the piezoelectric patch

C_v : Electric capacity of the piezoelectric patch

C_v' : Electric capacity per unit width of the piezoelectric patch

V_c : Tuning voltage applied on the piezoelectric stack actuator

e_{31} : Strain-Charge form piezoelectric coefficient

d_{31} : Strain-Charge form piezoelectric coefficient

ω_n : nth natural frequency of the beam

ω' : Excitation frequency

ξ : Damping ratio

C_o : Electrical capacity of the tuning circuit

R : Electrical resistance of the tuning circuit

1 Introduction

1.1 Background

Energy harvesting is a process that collects energy from ambient sources, such as dynamic motion of mechanical structures, wind and waves, and converting it to useful power, which can be stored for powering the electronic devices. This field has attracted much attention [1-4] over the past few decades due to the increasing demands of portable electronic devices and wireless sensor networks. Self-powering of those devices can be realized by effective harvesting energy from ambient sources and making good use of them, thus the small electronics devices will no longer be restricted by the limited life span of electrochemical batteries.

There are many ways to approach the energy harvesting process. Mitcheson et al [5] adopted an electrostatic generator using an un-sprung proof mass with a non-linear movement to build a Coulomb-force parametric generator, which harvests energy from low frequency, large amplitude movements. A electromagnetic vibration-to-electrical micro power generator was presented by Sari et al [6], which is able to generate steady power over a predetermined frequency range. Xie et al [7] developed an ocean wave energy harvester based on piezoelectric effects to harvest energy from the transverse wave motion of water particles. The use of piezoelectric patches attached on two horizontal cantilever plates and fixed on a vertical

rectangular column leads to efficient and practical energy harvesting from ambient wave pressures.

Piezoelectric materials are known as simple and economical smart materials which are applied in many industrial and manufacturing fields. The crystalline structure enabling them to transform mechanical strain energy into electrical charge (the direct piezoelectric effect) and, vice versa, to convert an applied electrical potential into mechanical strain (the reverse piezoelectric effect). To achieve energy harvesting in various applications, piezoelectric materials can be configured in many different ways [8]. The configuration of the piezoelectric energy harvester can be reformed through modification of piezoelectric materials, altering the electrode pattern, changing the poling and stress direction, layering the material to maximize the active volume, adding pre-stress to maximize the coupling and applied strain of the material, and tuning the resonant frequency of the energy harvester. For various applications in different structures, piezoelectric materials can be manufactured into many forms such as patches, thin films, stack cylinders and fibers. The most common type of piezoelectric materials used in energy harvesting applications is lead zirconate titanate, a piezoelectric ceramic, known as PZT. Owing to their ability to efficiently transform mechanical strain energy into electrical charge, high power generation density [9, 10] and flexible shape design that can fit in different structures for various applications, piezoelectric vibration-to-electricity converters have been widely employed as transducers for the energy harvesting application [11-16].

1.2 Literature review

In recent years, the piezoelectric energy harvesting has been studied and realized in different approaches. Priya [17] developed a theoretical model based on bending beam theory of bimorphs and equivalent circuit of capacitor for determination of generated electric power from wind energy using piezoelectric bimorph transducers. The calculated results were further verified to be excellent by an experiment using a prototype piezoelectric windmill consisting of ten piezoelectric bimorph transducers. Mateu and Moll [18] proposed an optimal design of bending beam structures of shoe inserts based on their former study [19]. They examined the combination of materials as well as the coupling mode and shape of the harvester, concluded that the maximum power output comes with a heterogeneous unimorph with a distributed load applied to a simply supported triangular beam. Rather than the conventional beam energy harvester, Erturk et al [20] employed a novel L-shaped beam-mass structure as a broadband energy harvesting system. This L-shaped structure can be tuned to have the first two natural frequencies relatively close to each other, which enables it to harvest energy from random or varying-frequency excitations. A piezoelectric coupled cantilever structure attached by a proof mass was developed by Xie et al [21] to achieve efficient energy harvesting from high-rise buildings. By investigating the dimensions and location of the piezoelectric patch, as well as the mass and radius of the attached mass, they found the optimal geometry of the proposed structure with the energy harvesting efficiency can even reach 28%. Ali et al [22] designed a single piezoelectric energy harvester embedded inside a bridge deck to generate energy from the motion of vehicles. The converted energy can be useful for wireless sensor networks for structural health monitoring of bridges by reducing or even eliminating the need for battery recharging.

With the growing attention on the field of energy harvesting using piezoelectric materials, some researches have been performed to increase the amount of energy harvested. Flexible piezoelectric materials with the ability to withstand large amounts of strain enable more mechanical energy available for transformation into electrical energy. In addition, by implementing a more efficient coupling mode, the energy harvested by piezoelectric materials can be considerably increased. The -31 mode, which is a force applied in the direction perpendicular to the poling direction, yields a lower coupling coefficient than the -33 mode, which is a force applied in the same direction with the poling direction. However, after a comparison between a piezoelectric stack operating in the -33 mode and a cantilever beam operating in the -31 mode of equal volumes, Baker et al [23] have observed that the cantilever harvests two orders of magnitude more power than the stack when subjected to the same force. Hence it is concluded that the -31 configuration proved most efficient in a small force, low vibration level environment. Roundy et al [24] also found that the operating system with -31 coupling mode harvests more power as the resonant frequency of it is much lower, which is more likely to be driven at resonance in a general situation. Moreover, through the analytical calculations conducted by Yang et al [25], it is shown that the output power is significantly increased when the driving frequency is close to a resonant frequency of the system. The reason is when a system operates at resonance, much greater displacements and strains are observed than operates slightly above or below resonance. Therefore, both the layout of piezoelectric materials and the configuration of operating system are playing important roles in energy harvesting.

To date, there have had generally two methods to increase the operating range of the energy harvesters [26], hence, enhancing the efficiency of energy harvesting process. The first is to

widen the bandwidth in the spectrum of the generator by combining with other equipment, such as non-linear springs, dampers and other oscillators[27]. Cornwell et al [28] proposed a tuned auxiliary structure consisting of a mechanical fixture and a PZT element, which can be attached to any vibrating system. By adjusting the parameters of the structure accurately, it can significantly improve the power generation. Xue et al [29] presented an approach for designing broadband piezoelectric harvesters by integrating multiple piezoelectric bimorphs with different aspect ratios into a system. It is illustrated that the bandwidth of a generator can be widened by connecting piezoelectric bimorphs in parallel and in series. In addition, by increasing or decreasing the number of piezoelectric bimorphs in parallel, the bandwidth of the generator can be shifted to the dominant frequency domain of the ambient vibration. Sari et al [30] reported a wideband electromagnetic micro power generator for wireless microsystems. The generator consists of serially connected cantilevers with various lengths which can efficiently scavenge energy and generate steady power over a predetermined frequency range. The length of the cantilevers increased gradually so that the cantilevers have various resonant frequencies and overlapping frequency spectra with the peak powers at similar but different frequencies. The proposed design leads to a widened bandwidth as well as an increase in the overall output power.

The second method is to tune the resonant frequency of the harvester to match the major frequency of the ambient vibration hence reach the resonant state of the harvester. Wu et al [31, 32] have proved that, for a piezoelectric coupled beam under a periodical dynamic point force, higher power-harvesting efficiency can be obtained when optimal design of the piezoelectric layer is applied and the excitation frequency is close to the resonant frequency. However, the ambient excitation frequency is usually unknown and variable. To realize the large power generation, many researchers have focused on developing a tuning mechanism [33-35], the

frequency tuning progress can be approached through mechanical tuning and electrical tuning. Mechanical tuning adjusts the resonant frequency by changing mechanical properties of the structure. Electrical tuning alters the resonant frequency by adjusting the electrical load.

1.2.1 Mechanical tuning methods

General mechanisms to realize frequency tuning are (i) changing dimensions, (ii) moving the center of gravity of the proof mass, (iii) variable spring stiffness, (iv) straining the structure.

Wu et al [36] presented a frequency adjustable energy harvester consists of a piezoelectric cantilever and a gravity center movable mass which has a fixed mass attached to the cantilever and a movable screw. The position of the center of gravity of the proof mass could be adjusted by changing the position of the movable screw. A fastening stud was used to fix the screw when tuning was finished. The resonant frequency of the device was tuned from 180 Hz to 130 Hz by moving the screw from one end to the other end and the output voltage increased correspondingly. Scheibner et al [37, 38] proposed a spectral vibration detection system with an array of eight comb resonators each has a different base resonant frequency. Each resonator comb is tuned by applying a tuning voltage to the electrodes through electrostatic softening (negative springs) to vary the total spring constant of the system. A maximum tuning voltage of 35 V is required for continuous resonance frequency tuning from 1 to 10 kHz. A frequency tunable comb resonator based on a closed-form approach of a curved comb finger contour is developed by Lee et al [39]. The curved finger generates a constant electrostatic stiffness or linear electrostatic force that is independent of the displacement of the resonator under a control voltage. Experimental results show that the resonant frequency of a laterally driven comb

resonator with 186 pairs of curved contour fingers has been reduced by 55% from the initial frequency of 19 kHz under a bias voltage of 150 V and the reduction is linearly proportional to the square of the control voltage as expected. It was concluded that the closed-form approach of the comb-finger profile can be applied to other comb-shape actuators for frequency control.

1.2.2 Electrical tuning methods

The basic principle of the electrical tuning is to change the electrical damping by adjusting the load, which shifts the power spectrum of the generator[26]. It is most feasible to control capacitive loads to realize electrical tuning since resistive loads reduce the efficiency of power transfer and load inductances are difficult to be varied.

Peters et al [40] proposed a tunable resonator for vibration energy harvesting. The resonant frequency tuning was realized by applying electrical potential to two piezoelectric actuators, thus increase the mechanical stiffness of the structure to further adjust the natural frequency of the rotational mass-spring system. Wu et al [41] developed a frequency tunable power harvesting device composed of a piezoelectric bimorph cantilever. The upper piezoelectric layer was used for frequency tuning while the lower layer was used for energy harvesting. The tunable bandwidth of this generator was 3 Hz between 91.5 Hz and 94.5Hz. The average harvesting output power of the generator with tuning was about 27.4% higher than that without tuning and the charging time of the generator was shortened by using the tuning system. The ratio of the thickness of the piezoelectric layer to the thickness of the substrate layer should be small to increase the tuning range.

Nevertheless, the power consumption during the frequency-tuning process needs to be considered. Roundy and Zhang [42] analyzed the feasibility of vibration-based generators with active tuning process. Due to the continuously power consumption even if the resonant frequency equals the ambient vibration frequency, the energy required to actively tune the device could not be compensated by the harvester. Hoffmann et al [43] proposed a self-adaptive energy harvesting system which is able to adapt its eigenfrequency to the operating conditions of power units. The tuning mechanism is based on a magnetic concept and incorporates a circular tuning magnet and a coupling magnet. From the experimental results, the net power can be considerably increased while the additional power is still required to adjust the eigenfrequency. However, it is noted that the energy consumed by the tuning mechanism should be as small as possible and must not exceed the increase in output power resulting from the frequency tuning. Therefore, the passive tuning has an advantage over the active tuning because the tuning process is switched off once the resonant frequency matches the ambient vibration frequency. A frequency self-tuning scheme for broadband vibration energy harvesting was presented by Lallart et al [44]. The system based on low-power frequency sensing relying on the phase between the base acceleration and piezoelement deflection, as well as a cost-effective stiffness tuning using switched piezomaterial, it has been validated that the exposed technique allows a fine tuning of the resonant frequency on a wide range. Inspired by their work, Eichhorn et al [45] investigated a piezoelectric energy-harvesting system, which is able to self-tune its resonant frequency in an energy-autonomous way. With the control unit set to perform frequency adjustments every 22s, a large power surplus was obtained. Through the use of a predefined look-up table, the power consumption of the tuning procedure is reduced. A passively self-tuning energy harvester for rotating applications was studied by Gu and Livermore [46, 47]. The harvester is comprised of

two beams: a relatively rigid piezoelectric generating beam and a narrow, flexible driving beam with a tip mass mounted at the end. They exploited the centrifugal force of a rotational system to provide tensile stress and change the resonant frequency of the harvester. With an optimized design, the resonant frequency of the harvester substantially matches the frequency of the rotation over a wide frequency range from 4 to 16.2 Hz.

Based on the fact that the vibrating beam varies its resonant frequency under compressive axial loads [48], Cabuz et al [49] realized resonant frequency tuning in the packaged device by applying an electrostatically activated axial force on a micromachined resonant beam. One end of the resonant was clamped on a fixed support while the other end was connected to a movable support. The moveable support could rotate around a torsion bar as a voltage was applied across two tuning electrodes. As an example of continuous tuning, The tuning range was 16 Hz based on a center frequency of 518 Hz with driving voltage from 0 to 16 V. Hu et al [50] theoretically investigated an axial preloading technique to adjust the behavior of a piezoelectric bimorph. Computational results indicate that resonance occurred when the natural frequency of the bimorph was adjusted to be adjacent to the external driving frequency by preloading. Leland and Wright [51] tested a tunable-resonance vibration energy scavenger which axially compressing a piezoelectric bimorph to lower its resonance frequency. It was demonstrated that the axial preload can adjust the resonance frequency of the simply supported bimorph to 24% below its unloaded resonance frequency.

1.3 Research objectives

From previous studies it can be seen that the frequency tunable energy harvesting has been approached in various methods. Nevertheless, with the application of amplifiers and complex electric circuits, the power consumption to realize the tuning process cannot be avoided and ignored, which will considerably decrease the efficiency of energy harvesting. The scope of my MSc study concentrates on accomplishing efficient energy harvesting with new developed self-tuning methods which can operate without external energy input. The contributions of this research work include the followings: (a) proposing an efficient energy harvesting methodology which can adjust its natural frequency automatically to match the major frequency of the ambient vibration lead to large power generation; (b) the frequency self-tuning is realized by a controlling voltage applied on a piezoelectric stack actuator to tune the natural frequency of the beam harvester; (c) two tuning methods with different closed-loop feedback circuits are developed to control the voltage on the piezoelectric stack actuator.

The thesis is organized as follows: Chapter 2 introduces a theoretical model of the energy harvester as well as an iteration numerical method to solve the forced vibration response with frequency self-tuning. To improve the energy harvesting efficiency, two different tuning methods are developed to reach the maximum power output in Chapter 3 and 4 respectively. Moreover, the finite element analysis is conducted to verify the effectiveness of the proposed design. The thesis closes with conclusions and future work in Chapter 5.

2 Theoretical model and methodology

The frequency self-tuning energy harvesting process is approached by applying a tuning voltage on a piezoelectric stack actuator at the end of a simply supported beam bonded with piezoelectric patches. The beam structure is shown in Fig. 2-1. The detailed dimensions of the beam harvester are given in section 2.1. Under the dynamic deformation of the beam subjected to ambient vibration, electrical charge is generated from the piezoelectric patches attached on the host beam to convert the input mechanical energy to electrical energy so as to approach the energy harvesting. To realize the self-tuning of the beam during vibration, the generated voltage from the piezoelectric patches is also used to power the piezoelectric stack actuator, which will generate a compressive axial force to the beam to tune the natural frequency of it automatically. It is noted that with the increasing voltage generation from the piezoelectric patches, the tuning voltage applied on the piezoelectric stack actuator as well as the compressive axial force generated by the piezoelectric stack actuator will keep growing, which continuously tuning the natural frequency of the beam getting close to the major excitation frequency of the ambient vibration leading to large power generation.

To describe this energy harvesting and the self-tuning process, a mathematical model is presented to calculate the dynamic response of the beam harvester as well as the output electric charge and voltage from the piezoelectric patches corresponding to varying axial force during the self-tuning process. It is noted that as a result of transient vibration with variable axial force

applied on the beam structure, the natural frequency and vibration mode shapes of the beam will keep changing at different time points, which means the full vibration response of beam should be recalculated accordingly. To simulate and explain the changing natural frequency and vibration mode shapes of the beam harvester during the transient self-tuning process, an iteration numerical method is developed and explained in section 2.2.

2.1 A theoretical model of the beam energy harvester with compressive axial force

As shown in Fig. 2-1, two piezoelectric patches with length *a* is mounted on the middle part of upper and lower surfaces of the simply supported beam with a length of *L*. L_1 denotes the distance from the left supported end of the beam to the left end of the piezoelectric patches. The width of the host beam and the piezoelectric patches is *b*, while the thickness is *h* and h_1 respectively. The beam harvester is working with ambient vibration which can be set to be $f(x,t)$ as a simple representative. In Chapter 3 and 4, a base motion excitation and a dynamic point load will be used separately to study the forced vibration response of the beam energy harvester under ambient excitation.

According to the Euler-Bernoulli beam theory, the governing equation of the simply supported beam under ambient excitation and compressive axial force *P* can be expressed as:

$$EI\frac{\partial^4 w(x,t)}{\partial x^4}+\rho bh\frac{\partial^2 w(x,t)}{\partial t^2}+P\frac{\partial^2 w(x,t)}{\partial x^2}=f(x,t) \qquad (2-1)$$

where $w(x,t)$ is the vibration deflection of the host beam along its length direction, *x*, at time, *t*. E and ρ are the Young's modulus and density of the host beam, respectively. I is the moment of inertia of the beam. The axial force, P, which is generated by the tuning voltage applied on the piezoelectric stack actuator is used to realize the self-tuning process. The generation of the axial force P and the self-tuning process is explained as below.

When a bending motion takes place on the piezoelectric patches attached on a beam that is subjected to external excitation, the total electric charge generated on the surfaces of one of the piezoelectric patches, which is assumed to be completely bonded on the bending beam, is found to be [52]:

$$Q(t) = -e_{31}\int_{L_1}^{L_2} b\left(\frac{h+h_1}{2}\right)\frac{\partial^2 w(x,t)}{\partial x^2}\,dx \qquad (2-2)$$

where e_{31} is the piezoelectric constant, $L_2 = L_1 + a$. The corresponding voltage generated on the piezoelectric patches can be written as [53]:

$$V(t) = \frac{Q(t)}{C_v} = -\frac{e_{31}(h+h_1)}{2C_v'}\int_{L_1}^{L_2}\frac{\partial^2 w(x,t)}{\partial x^2}\,dx \qquad (2-3)$$

where C_v is the electric capacity of the piezoelectric patch and C_v' is the electric capacity per unit width of the piezoelectric patch ($C_v' = C_v/b$).

The generated voltage from piezoelectric patches will be used to power the piezoelectric stack actuator through two different electrical circuits which will be further explicated in Chapter 3 and 4. The tuning voltage applied on the piezoelectric stack actuator, $V_c(t)$, is inducing axial

stress along the piezoelectric stack actuator to tune the natural frequency of the beam harvester can be expressed as [54]:

$$\sigma = e_{33} V_c(t)/h_2 \qquad (2-4)$$

where h_2 is the thickness of one layer of the piezoelectric stack actuator. The axial force on the beam generated by the piezoelectric stack actuator is hence:

$$P = \sigma A_1 \qquad (2-5)$$

where A_1 is the cross section area of the piezoelectric stack actuator.

To solve the dynamic deflection $w(x,t)$ in Eq. (2-1), the forced vibration solution of the beam harvester can be determined using the mode superposition principle, the deflection of the beam is assumed as:

$$w(x,t) = \sum_{n=1}^{\infty} W(n,x) q(n,t) \qquad (2-6)$$

where $W(n,x)$ is the nth mode shape function and $q(n,t)$ is the generalized coordinate in the nth mode ($n=1, 2, \ldots, \infty$).

In the space domain, for a certain mode of the classical elastic beam model, the piezoelectric coupled beam is simply separated into three sections, by considering the piezoelectric bonded area, 2, connected with the non-bonded beam sections 1 and 3. Based on

the Euler-Bernoulli beam theory, the vibration governing equation for three sections can be expressed as:

$$EI\frac{d^4W_1(x)}{dx^4}+P\frac{d^2W_1(x)}{dx^2}-\rho bh\omega^2W_1(x)=0 \qquad (0\le x\le L_1)$$

$$(EI)'\frac{d^4W_2(x)}{dx^4}+P\frac{d^2W_2(x)}{dx^2}-(\rho bh+2\rho' bh_1)\omega^2W_2(x)=0 \qquad (L_1\le x\le L_2)$$

$$EI\frac{d^4W_3(x)}{dx^4}+P\frac{d^2W_3(x)}{dx^2}-\rho bh\omega^2W_3(x)=0 \qquad (L_2\le x\le L) \qquad (2-7)$$

where EI is given as, $EI=Ebh^3/12$, and $(EI)'=EI+E_pb\frac{(h+2h_1)^3-h^3}{12}$, E_p and ρ' are the equivalent Young's modulus and density of the piezoelectric patch. ω is the natural frequency of the beam harvester.

The solution of $W_1(x)$~$W_3(x)$ are the vibration mode functions corresponding with the three sections of the beam and can be obtained as:

$$W_1(x)=C_1cosk_1x+C_2sink_1x+C_3coshk_2x+C_4sinhk_2x$$

$$W_2(x)=C_5cosk_3x+C_6sink_3x+C_7coshk_4x+C_8sinhk_4x \qquad (2-8)$$

$$W_3(x)=C_9cosk_1x+C_{10}sink_1x+C_{11}coshk_2x+C_{12}sinhk_2x$$

where $k_1=\left\{\frac{P}{2EI}+\left[\frac{P^2}{4(EI)^2}+\frac{\rho bh\omega^2}{EI}\right]^{1/2}\right\}^{1/2}$, $k_2=\left\{\frac{-P}{2EI}+\left[\frac{P^2}{4(EI)^2}+\frac{\rho bh\omega^2}{EI}\right]^{1/2}\right\}^{1/2}$,

$$k_3 = \left\{\frac{P}{2(EI)'} + \left[\frac{P^2}{4(EI)'^2} + \frac{(\rho bh + 2\rho' bh_1)\omega^2}{(EI)'}\right]^{1/2}\right\}^{1/2}, \quad k_4 = \left\{\frac{-P}{2(EI)'} + \left[\frac{P^2}{4(EI)'^2} + \frac{(\rho bh + 2\rho' bh_1)\omega^2}{(EI)'}\right]^{1/2}\right\}^{1/2}.$$

$C_1 \sim C_{12}$ are constants, which can be solved with certain boundary conditions. For the simply supported piezoelectric coupled beam, there are four boundary conditions and eight continuity conditions:

$$x = 0:\ W_1(x) = 0, \frac{d^2W_1(x)}{dx^2} = 0 \tag{2-9}$$

$$x = L_1: W_1(x) = W_2(x), \frac{dW_1(x)}{dx} = \frac{dW_2(x)}{dx}$$

$$EI\frac{d^2W_1(x)}{dx^2} = (EI)'\frac{d^2W_2(x)}{dx^2} + 2M_e$$

$$EI\frac{d^3W_1(x)}{dx^3} = (EI)'\frac{d^3W_2(x)}{dx^3} \tag{2-10}$$

$$x = L_2: W_2(x) = W_3(x), \frac{dW_2(x)}{dx} = \frac{dW_3(x)}{dx}$$

$$EI\frac{d^2W_3(x)}{dx^2} = (EI)'\frac{d^2W_2(x)}{dx^2} + 2M_e$$

$$EI\frac{d^3W_3(x)}{dx^3} = (EI)'\frac{d^3W_2(x)}{dx^3} \tag{2-11}$$

$$x = L:\ W_3(x) = 0, \frac{d^2W_3(x)}{dx^2} = 0 \tag{2-12}$$

where M_e is the bending moment induced at the two ends of the piezoelectric patches, $M_e = S \times h/2$, S is the shear force generated at the interface between the piezoelectric patch and the host beam, $S = Ehb/(\Psi + \alpha) \times d_{31}V/h$, $\Psi = Eh/E_p h_1$ [55].V is the voltage generated on the surfaces of piezoelectric patches corresponding with certain vibration mode. For a bending beam, $\alpha = 6$, and d_{31} is the piezoelectric charge coefficient. Substituting Eq. (2-8) into boundary conditions (2-9) to (2-12) leads to twelve linear equations, from which we can obtain the solution of *n*th natural frequency of beam, ω_n, and its corresponding normal mode *W(n,x)*. It is noted that during the self-tuning process, the axial force varies with the increment of the generated voltage from the piezoelectric patches as well as the tuning voltage on the piezoelectric stack actuator. Those effects lead to a continuum changing of the nature of the beam harvester at different time points. To solve the transient forced vibration response of the beam harvester in time domain, $q(n, t)$, an iteration numerical method is proposed and discussed in detail in the next section.

2.2 Iteration numerical method solving the forced vibration response with continuous frequency-tuning

It is assumed that the structure is at rest initially. During the frequency-tuning process, according with the increasing generated voltages on the piezoelectric patches, the tuning voltage applied on the piezoelectric stack actuator will be increased leading to a variable axial force. Under this changing axial force, the natural frequency and vibration response of the beam harvester keeps changing. Due to this transient vibration characteristic, we adopt an iteration numerical method [56] in addition to the traditional Duhamel Integral to derive an accurate vibration solution of the beam harvester subjected to external excitation and the variable axial force.

To solve the accurate vibration response, the dynamic progress during the vibration is separated into many short periods to represent the iteration steps. With the assumption that the structure is at rest initially, the initial deflection $w(x,t)$ and velocity $\frac{\partial w(x,t)}{\partial t}$ at any location of beam at *t=0*, are zero, where *x* is the location on the beam along its length direction.

The iteration step length of each short time period, $t_i \sim t_{i+1}$, is $\Delta t = t_{i+1} - t_i$, where i is iteration step number, $1 \leq i < \infty$. For any short period, $t_i \sim t_{i+1}$, the full vibration response can be divided into two parts. The first part is the vibration response induced by the dynamic point load applied to the beam during the time period $t_i \sim t_{i+1}$. The second part is the free vibration response owing to the initial condition at t_i, which is determined by the final vibration response at the end of the previous time period $t_{i-1} \sim t_i$, at t_i.

Since the generated electric charge depends on the real-time mechanical strain on the piezoelectric patches, more accurate vibration solution should be obtained by shorter iteration step length. For the first iteration step, $t_1 \sim t_2$, the initial conditions are $w(x,t) = \frac{\partial w(x,t)}{\partial t} = 0$, and then the forced vibration response can be solved by:

$$w(x,t) = \sum_{n=1}^{\infty} W(n,x) q_1(n,t) \qquad (2-13)$$

$$= \sum_{n=1}^{\infty} W(n,x) \frac{1}{\rho b h T_n \omega_d} \int_0^{t-t_1} \int_0^L f(x, \tau + t_1) W(n,x) \exp[-\xi \omega_n (t - t_1 - \tau)] \sin[\omega_d (t - t_1 - \tau)] \, dx \, d\tau,$$

$$(t_1 \leq t \leq t_2)$$

where $q_1(n,t)$ is the generalized coordinate in the *n*th mode from Duhamel Integral at the first time period/iteration step, $t_1 \sim t_2$. ω_n is the *n*th natural frequency of the beam harvester. $\omega_d = \sqrt{1-\xi^2}\omega_n$ is the damped frequency of the beam considering the damping ratio, ξ. $T_n = \int_0^L W^2(n,x)\,dx$. It is noted the natural frequency of the beam, ω_n, keeps changing during the tuning process.

For the second step of iteration, the free vibration response in the second period, $t_2 \sim t_3$, can be written as:

$$w_{free}(x,t) = \sum_{n=1}^{\infty} W(n,x)(A_n cos\omega_n t + B_n sin\omega_n t), \quad (t_2 \le t \le t_3) \quad (2-14)$$

where the constants A_n and B_n can be found by the final solution of previous time period, $q_1(n,t)$ and $\frac{dq_1(n,t)}{dt}$ at $t = t_2$, given by Eq. (2-13), as initial conditions for the second period $t_2 \sim t_3$. Thus we have,

$$(A_n cos\omega_n t_2 + B_n sin\omega_n t_2) = q_1(n,t_2)$$

$$-A_n\omega_n\, sin\omega_n t_2 + B_n\omega_n\, cos\omega_n t_2 = \frac{dq_1(n,t)}{dt}\Big|_{t=t_2}. \quad (2-15)$$

Accumulating Eq. (2-14) to the forced vibration response solved by Duhamel Integral at the time duration of $t_2 \sim t_3$, the full vibration solution of the second time period/iteration step can be obtained as:

$$w(x,t) = \sum_{n=1}^{\infty} W(n,x) q_2(n,t) \qquad (2-16)$$

$$= \sum_{n=1}^{\infty} W(n,x) \left\{ \frac{1}{\rho b h T_n \omega_d} \int_0^{t-t_2} \int_0^L f(x,\tau+t_2) W(n,x) \exp[-\xi\omega_n(t-t_2-\tau)] \begin{matrix} A_n cos\omega_n t + B_n sin\omega_n t + \\ sin[\omega_n(t-t_2-\tau)] dx\, d\tau \end{matrix} \right\},$$

$$(t_2 \le t \le t_3)$$

where $q_2(n,t)$ is the generalized coordinate in the *n*th mode at the second time duration $t_2 \sim t_3$.

Following the same iteration process, the transient vibration response at any time period of $t_i \sim t_{i+1}$, can be calculated step by step to derive the solution:

$$w(x,t) = \sum_{n=1}^{\infty} W(n,x)\, q_i(n,t) \qquad (2-17)$$

$$= \sum_{n=1}^{\infty} W(n,x) \left\{ \frac{1}{\rho b h T_n \omega_d} \int_0^{t-t_i} \int_0^L f(x,\tau+t_i) W(n,x) \exp[-\xi\omega_n(t-t_i-\tau)] \begin{matrix} A_n cos\omega_n t + B_n sin\omega_n t + \\ sin[\omega_n(t-t_i-\tau)]\, dx d\tau \end{matrix} \right\},$$

$$(t_i \le t \le t_{i+1})$$

where A_n and B_n are given as follows from the iteration:

$$B_n = \frac{\frac{dq_{i-1}(n,t)}{dt}|_{t=t_i} cos\omega_n t_i + q_{i-1}(n,t_i)\omega_n sin\omega_n t_i}{\omega_n sin^2\omega_n t_i + cos^2\omega_n t_i}$$

$$A_n = \frac{q_{i-1}(n, t_i) - B_n sin\omega_n t_i}{cos\omega_n t_i}. \quad (2-18)$$

With the derived *w(x,t)* in Eq. (2-17), we can obtain the generated charge $Q(t)$ and voltage $V(t)$ on the piezoelectric patches from Eqs. (2-2) and (2-3). During the tuning process, before reaching the resonant state, both the tuning voltage and the axial force keep growing. The generated power on the piezoelectric patches is increasing as well. We adopt the root mean square (RMS) value to evaluate the output electric power for a time period *T*. From the Eqs. (2-2) and (2-3), the output electric power from the two piezoelectric patches at time t $(0 < t < T)$ is:

$$P_e(t) = V(t)I_e(t) = V(t)2\frac{dQ(t)}{dt} \quad (2-19)$$

where $I_e(t)$ is the electric current generated on the piezoelectric patches. Hence, the RMS value of the output electric power from time *0* to *T* can be expressed as:

$$P_e^{rms} = \sqrt{\frac{1}{T}\int_0^T P_e^2(t)dt} \quad (2-20)$$

The difference of the RMS value of the output electric power with or without frequency-tuning process will be compared in Chapter 3 and 4 to prove the efficiency of the proposed self-tuning energy harvesting.

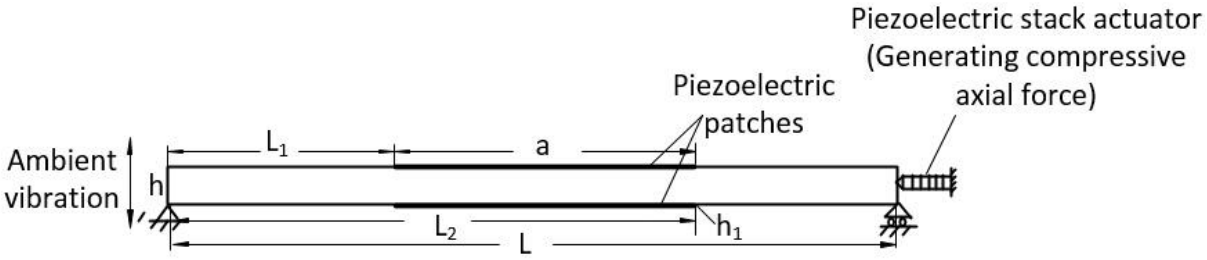


Fig. 2-1 A simply supported beam energy harvester with compressive axial force.

3 Self-tuning with a feedback filtering circuit

This efficient energy harvesting system consists of a simply supported beam energy harvester coupled with piezoelectric patches, a filtering circuit and a piezoelectric stack actuator shown in Fig. 3-1. The ambient vibration of the system is treated as a base motion excitation on the energy harvester. It can be studied by setting an excitation of a harmonic sinusoidal wave as a simple representative. Therefore, the harmonic base motion is set to be $w_g(t) = Ysin\omega' t$, where Y is the amplitude of the base displacement, ω' is the angular frequency of the base motion. The distributing inertia force on the beam structure can be written as, $f(x,t) = -\rho bhY\omega'^2 sin\omega' t$. At the initial stage of the beam harvester vibration excited by the base excitation, the electrical charge and voltage generate on the piezoelectric patches. Through the feedback filtering circuit, the axial force will be produced by the piezoelectric stack actuator and applied to the right end of the beam harvester. The value of axial force is determined by the amplitude of the output voltage generated on the piezoelectric patches. Under this axial force, the first natural frequency of the beam will be tuned to get close to the excitation frequency. When the first natural frequency of the beam harvester is closer to the excitation frequency, the vibration deflection of the beam harvester and the tuning voltage applied on the piezoelectric stack actuator will further increase to keep tuning the first natural frequency till the resonance with the maximum power generation.

3.1 Principle of the feedback filtering circuit

The filtering circuit based on the combinations of resistors (R), inductors (L) and capacitors (C) is shown in Fig. 3-1. It connected to the piezoelectric patches through an alternating current (AC)/direct current (DC) converter circuit (diode bridge circuit) which converts the sinusoidal voltage signal generated from the piezoelectric patches to a DC voltage output. Therefore, the generated voltage from Eq. (2-3) will become $V_o(t) = |V(t)|$ after the diode bridge circuit. The filtering circuit will further remove the dynamic components from the signal and provide a smooth and stable tuning voltage V_c, which is applied to the piezoelectric stack actuator to generate the axial force calculated by Eq. (2-4) and (2-5).

3.2 Numerical simulations and discussions

In this section, numerical simulations are conducted based on the proposed theoretical beam model and numerical method in Chapter 2. The generated voltage and output electric power on the piezoelectric patches are calculated. From the simulations, we made a comparison between the RMS values of output electric power with/without frequency-tuning. Furthermore, an optimal design of the length of piezoelectric patches is developed to achieve larger RMS value of power generation. The dimensions and material properties of the piezoelectric coupled beam used in the simulations are listed in Table 3-1.

Fig. 3-2 illustrates the generated voltage and output electric power on piezoelectric patches without self-tuning process. The resulting motion exhibits a phenomenon known as beating, which usually occurs when the forcing frequency is close to the natural frequency of the beam.

From the simulation, the first natural frequency of beam harvester is 152 rad/s, while the excitation frequency is 130 rad/s. Thus the beating frequency is (152-130)/2 rad/s, and the beating cycle is around 0.57s. Without the self-tuning process, the RMS value of the output electric power generated on the piezoelectric patches in the 1st second of vibration is 7.2 mW.

Fig. 3-3 presents an efficient self-tuning process with the axial force induced by the tuning voltage applied on the piezoelectric stack actuator. During the self-tuning, the first natural frequency of the beam harvester is tuned getting close to the excitation frequency. When the first natural frequency of the beam harvester is closer to the excitation frequency, the vibration deflection of the beam harvester and the voltage from piezoelectric patches will further increase to realize larger electrical power output as well as the tuning of the first natural frequency till the resonance. It should be noted that, considering the failure of the materials due to significantly large deflection at the resonance, the largest lateral displacement of the beam harvester with 1m length is constrained within 4 cm in the simulations. It is seen from Fig. 3-3, after 0.38s, the tuning process is completed while the largest deflection of the beam reaches the restriction giving the maximum output electric power without breaking the beam harvester. The generated voltage after frequency-tuning is 40 V, which is two times higher than the maximum beating voltage output without frequency-tuning shown in Fig. 3-2. The RMS value of the output electric power with the self-tuning process in the 1st second of the vibration is 72.9 mW, which is 10 times of the counterpart without tuning process (7.2 mW), even if the largest deflection of the beam is restricted.

From the results above, it can be seen that the proposed energy harvesting system provides an efficient self-tuning method. The feedback filtering circuit and the piezoelectric stack actuator

can operate without external energy input, which fulfill the prerequisite of an efficient energy harvesting system.

Finally, the effect of the length of piezoelectric patches on the output electric power is studied, and an optimal design of the piezoelectric patches is proposed. Since it is a simply supported beam structure, the largest strain will always occurs at the middle span deflection. The output electric power on the piezoelectric patches is dependent upon charge and capacity of the piezoelectric patches. Meanwhile, the charge on the piezoelectric patches depends on the length and the curvature of the area covered by the patches. With an increase in the length of the piezoelectric patches, the average curvature on the piezoelectric patches would be reduced, and the capacitance of the piezoelectric patches will increase, leading to the possible decrease of the generated voltage on the piezoelectric patches, although the total charge on the piezoelectric patches keeps increasing. For the proposed beam model, with different length of piezoelectric patches mounted on the middle part of it, RMS values of the output electric power during the 1st second of the vibration are calculated and shown in Figure 3-4. It can be seen that, with constant width and thickness, the optimal length of the piezoelectric patches is 0.5 m.

3.3 Conclusions

In this chapter, an efficient self-tuning energy harvesting method is proposed. Under harmonic base excitation in simulations, this energy harvester consists of a simply supported beam bonded with piezoelectric patches can efficiently self-tune its first natural frequency getting close to the excitation frequency to achieve the maximum electric power output within 0.4s, while deflection of the beam harvester is restricted. The outcome proves the efficiency of this energy harvesting

system, with 10 times RMS value of the output electric power comparing to the one without tuning process. In addition, a parameter study of the length of piezoelectric patches is conducted to achieve the maximum RMS value of the output electric power. The optimal length of the piezoelectric patches with thickness of 0.3 mm, which are attached at the middle of the host beam, is found to be 0.5 m, while the length and thickness of the host beam is 1 m and 1 cm, respectively.

Table 3-1 Dimensions and material properties of the piezoelectric coupled beam.

Parameter	Host beam (aluminum)	Piezoelectric patches
Young's modulus (N m^{-2})	$E=69\times10^{9}$	$E_p=78\times10^{9}$
Mass density (kg m^{-3})	2.8×10^{3}	7.5×10^{3}
e_{31} (C m^{-2})	-	-2.8
e_{33} (C m^{-2})	-	10
d_{31} (C N^{-1})	-	-1.28×10^{-10}
C_v (μF)	-	0.98 for a piezoelectric patch with dimensions of 0.02m×0.4m×0.0003m
L (m)	1	-
L_1 (m)	0.3	-
a (m)	0.4	-
h (m)	0.01	-
h_1 (m)		0.0003
b (m)	0.02	-

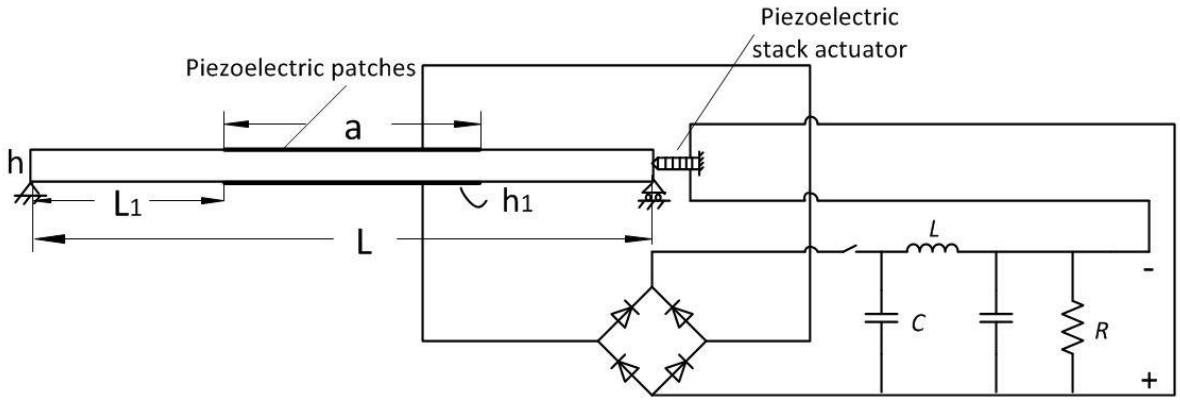


Fig. 3-1 Schematic diagram and geometries of proposed energy harvester.

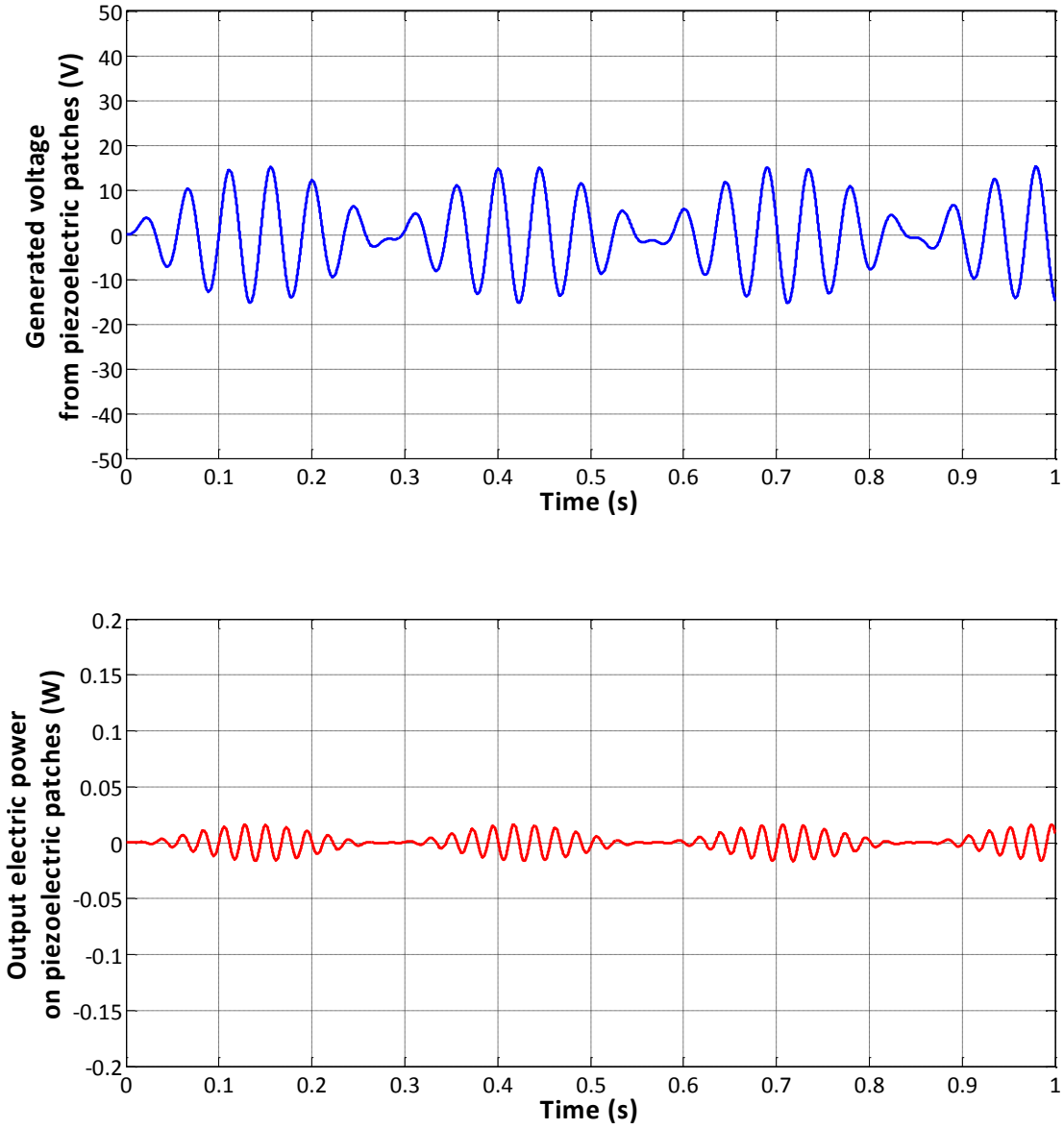


Fig. 3-2 Generated voltage and output electric power on piezoelectric patches without self-tuning.

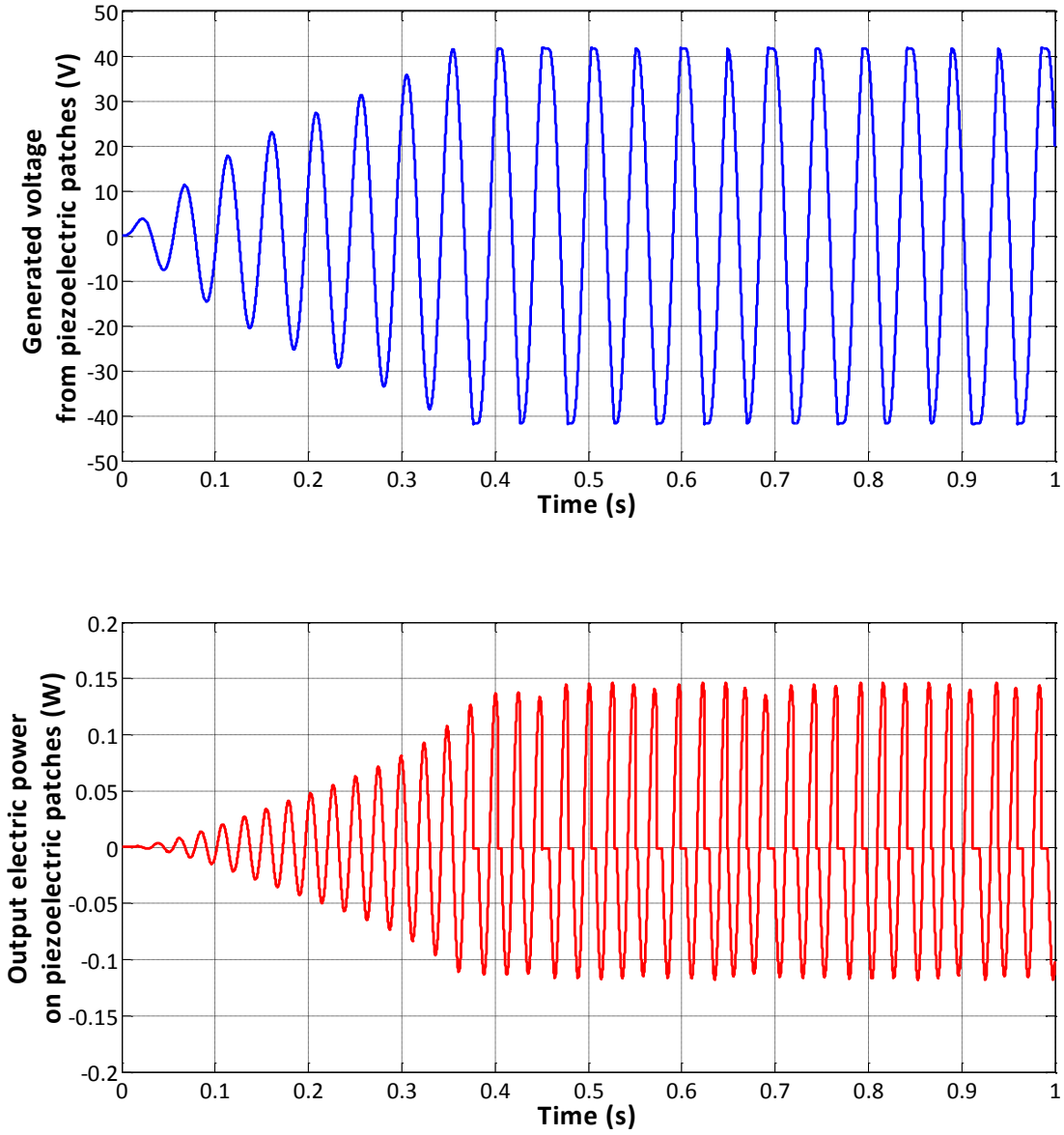


Fig. 3-3 Generated voltage and output electric power on piezoelectric patches with self-tuning.

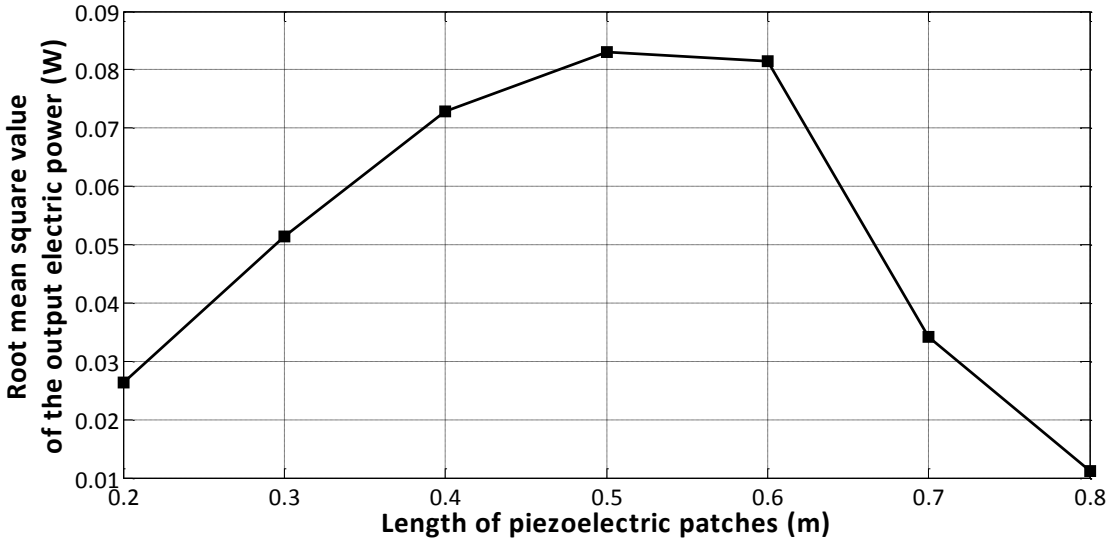


Fig. 3-4 RMS value of the output electric power versus different length of piezoelectric patches.

4 Self-tuning with a tuning capacitor

Following the study of the efficient energy harvesting system with a feedback filtering circuit [57], further research is conducted to achieve the self-tuning energy harvesting with a tuning electrical circuit which provides more stable tuning voltage and feasible controlling technique. In this chapter, a tuning circuit with a small tuning capacitor is used to determine the tuning voltage applied on the piezoelectric stack actuator. The tuning capacitor is charged by the piezoelectric patches through a diode bridge. It is assumed that the tuning circuit has less effect on the voltage output on the piezoelectric patches. As a result of the diode bridge, the electric current flow can only be in one direction so that the tuning capacitor can be charged without any discharge process. When the converted DC voltage is larger than the voltage on the tuning capacitor, the capacitor will be charged. Otherwise, the capacitor cannot be further charged owing to the diode bridge circuit. The charging process of the tuning capacitor is discontinuous as illustrated in Fig. 4-1. Compared with the previous design using the voltage on the filtering circuit as the tuning voltage, the charged voltage on the tuning capacitor is more stable which provides better management of the self-tuning process. The detailed design of the electrical circuits and controlling method will be explained in the following section.

4.1 Design of the tuning circuit

The proposed energy harvesting system consists of a simply supported beam energy harvester coupled with piezoelectric patches, a filtering circuit, a tuning circuit, an energy harvesting circuit and a piezoelectric stack actuator shown in Fig. 4-2(a). The detailed dimensions of the harvester are given in Table 4-1. The ambient vibration of the system is treated as a dynamic load applying on L_3 from the left end of the beam harvester. To realize the self-tuning process of the harvester during the vibration, the generated voltage from the piezoelectric patches is also used to charge the tuning capacitor through a diode bridge circuit. The charged voltage on the tuning capacitor will be applied to the piezoelectric stack actuator generating a compressive axial force on the beam harvester so as to tune the natural frequency of it automatically during the vibration. It is noted that with the increasing charged voltage on the tuning capacitor, the compressive axial force generated by the stack actuator will keep growing, which continuously tuning the natural frequency of the beam harvester getting close to the excitation frequency. When the beam harvester reaches the resonant state, the vibrating deflection as well as the generated charge on the piezoelectric patches reaches the peak value. To avoid the extremely large deflection of the beam and the over-tuning that the natural frequency of the beam harvester passing the excitation frequency, the charging process of the tuning capacitor is controlled by a filtering circuit, which is connected with the harvester to pick up its generated peak voltage. From Fig. 4-2(a), it is seen that a voltage controlled electronic switch is connected with the tuning circuit to control the charging of the tuning capacitor, and it is closed. During the tuning process, when the tuned natural frequency of the beam harvester is close to the excitation frequency, large deflection of the beam harvester will lead to high voltage generated on the piezoelectric patches. Once the deflection reaches to the largest restriction without breaking the

harvester, the peak voltage generated on the piezoelectric patches is picked up by the filtering circuit and turn off the electronic switch, hence the charging circuit of the tuning capacitor is cut off then. An insulating layer is mounted on one side of the electronic switch to avoid short-connection of the filtering circuit. In this case, no matter what the excitation frequency is, as long as it is smaller than the first natural frequency of the beam harvester, the harvester is always self-tuned close to its resonant state with large deflection and electrical power output before the tuning circuit is cut off. With a certain excitation frequency, the maximum charged voltage on the tuning capacitor will always keep a certain value leading to a constant axial forced generated by the piezoelectric stack actuator, and the tuned natural frequency of the beam harvester will be a constant value close the excitation frequency as well, thus the vibration of the harvester will stay close to the resonant state.

To solve the charged voltage on the tuning capacitor, the charging period T is separated into m small discrete sections to calculate the charged voltage on the tuning capacitor at certain time t_i $(1 \le i \le \infty, and\ t_1 = 0)$. The step length of each time section is $t_i - t_{i-1}$. The equivalent electrical resistance of the circuit is R and the capacitance of the capacitor is C_o. Let $V_o(t) = |V(t)|$ denotes the converted output DC voltage and $V_c(t)$ is the voltage on the tuning capacitor. Therefore, the differential equation of the charging process can be expressed as:

$$\begin{cases} V_o(t_i) > V_c(t_{i-1}):\ RC_o \dfrac{\partial V_c(t)}{\partial t} + V_c(t) = V_o(t) \\ V_o(t_i) \le V_c(t_{i-1}): V_c(t_i) = V_c(t_{i-1}) \end{cases} \qquad (t_{i-1} < t < t_i) \qquad (4-1)$$

By solving Eq. (4-1), the voltage on the tuning capacitor can be obtained:

$$\begin{cases} V_o(t_i) > V_c(t_{i-1}): V_c(t_i) = \dfrac{V_o(t_{i-1})e^{\frac{t_{i-1}}{RC_o}} + V_o(t_i)e^{\frac{t_i}{RC_o}}}{2RC_o}(t_i - t_{i-1})e^{\frac{-t_i}{RC_o}} + G_i e^{\frac{-t_i}{RC_o}} \\ V_o(t_i) \le V_c(t_{i-1}): V_c(t_i) = V_c(t_{i-1}) \end{cases} \quad (4-2)$$

where G_i is a constant value solved by considering the initial condition of Eq. (4-1) at $t = t_{i-1}$ and can be written as:

$$G_i = V_c(t_{i-1})e^{\frac{t_{i-1}}{RC_o}} \quad (4-3)$$

From the initial conditions, $V_c(t_1 = 0) = 0$, the voltage on the tuning capacitor $V_c(t)$ can be solved sequentially. By substituting Eq. (4-2) into Eq. (2-4) and (2-5), the axial force is hence determined to tune the natural frequency of the beam harvester.

4.2 Numerical simulations and discussions

In this section, numerical simulations are conducted based on the proposed theoretical model and the iteration numerical method in Chapter 2 to realize the energy harvesting with the self-tuning process. The generated voltage and the output electric power from the piezoelectric patches as well as its RMS value under certain excitation point load with/without tuning process are calculated and compared. The dimensions and material properties of the energy harvesting system used in the simulations are listed in Table 4-1. To avoid the failure of materials due to the significantly large deflection of the beam harvester while approaching the resonant state, the largest deflection of the beam harvester is restricted during the tuning process. As discussed in section 4.1, this restriction is realized by cutting off the charging of the tuning capacitor by the filtering circuit shown in Fig. 4-2(c) so as to restrict the axial force generated by the actuator and

avoid the over-tuning of the harvester's natural frequency. Moreover, the parameter studies of the length and thickness of the piezoelectric patches, the capacitance of the tuning capacitor, and the equivalent electric resistance of the tuning circuit are conducted leading to the optimal design of the proposed energy harvesting system with higher power output. With a compressive load from the actuator used in this research, the tuning process works for any dynamic external excitation with the frequency that is smaller than the 1st natural frequency of the harvester before tuning.

To investigate the self-tuning process of the beam harvester, the excitation frequency and amplitude of the dynamic point load are set to be 140 rad/s and 2.5 N in all simulations. Damping effect is considered in the simulations with the equivalent damping ratio of 2%. The iteration step length is 0.001s. (The discussion of the iteration convergence with the iteration step length is given Fig. 4-5) For the proposed simply supported beam coupled with piezoelectric patches, the first natural frequency is calculated as 154.1 rad/s. The tuning process is accomplished when the natural frequency of the beam harvester is close to the excitation frequency leading to the largest restricted deflection of the beam. Considering the design factor of safety for brittle materials under dynamic loading as 5 [58], the acceptable stress applied on piezoelectric patches cannot be larger than 70 MPa. In this case, based on the relationship between the stress and deflection of a Euler-Bernoulli beam model, $\sigma = -E\frac{(h+2h_1)}{2}\frac{\partial^2 w(x,t)}{\partial x^2}$, the deflection restriction of the beam is chosen as 4 cm in this study on the 0.75 m length beam harvester, when the excitation frequency is close to the first natural frequency of the beam. With certain dimensions given in Table 4-1, the amplitude of the voltage generated on the piezoelectric patches with the largest deflection restriction of 4 cm is 43.30 V, which is used to

cut off the tuning circuit by the electro-switch when the tuning is accomplished. In this case, the tuning process works for different excitation frequencies, which are usually unknown before the tuning. Under the largest axial force generated by the piezoelectric stack actuator after tuning, the beam harvester reaches its resonant state with the natural frequency tuned to be 140.83 rad/s, the amplitude of the voltage generated on the piezoelectric patches is 43.30 V. Fig. 4-3 illustrates the transverse displacement at the middle of the beam harvester of 3.98 cm after tuning and 0.76 cm without tuning, respectively. The generated voltage and the output electric power from the piezoelectric patches for a period of 4 seconds with and without tuning are given in Fig. 4-4. It is seen that the self-tuning process is completed around 2 seconds, and the amplitude of generated voltage (43.30 V) is 5.1 times of the one (8.49 V) without tuning. Considering the damping effect, the beam harvester works on its steady state with the largest power generation after the tuning. The RMS value of the output electric power with self-tuning at steady state is 0.1389 W, which is 26.2 times of the one without tuning (0.0053 W). From the results above, it can be seen that the proposed energy harvesting system provides an efficient self-tuning to significantly improve the power generation from the harvester. The new design of the tuning circuit and the piezoelectric stack actuator can realize the efficient tuning for different excitation frequencies and operate without any external energy input. Fig. 4-5 shows the convergence of the RMS value of the output power from the harvester with different iteration step length. It is seen that the step length of 0.001s is small enough giving accurate RMS power output value.

To further increase the generated power of the proposed beam harvester, parameter studies are conducted. First, the effect of the thickness of the piezoelectric patches on the power generation is studied and shown in Fig. 4-6. The natural frequency of the beam harvester after tuning, the peak generated voltage from the piezoelectric patches as well as the RMS value of the

output electric power during the period of steady state (3s-4s) after tuning are provided in Table 4-2. It has to be noted that, for the purpose of limiting the deflection of the beam harvester within a reasonable range (4 cm), in some cases, the beam harvester has not reached the exact resonant state after tuning. This tuning restriction is realized by cutting off the charging of the tuning capacitor through the filtering circuit. From Fig. 4-6, it is obviously that, with constant length (0.3m) of the piezoelectric patches, thicker piezoelectric patches lead to greater power generation. The RMS value of output electric power can reach 0.1389 W at the steady state when the thickness of the piezoelectric patches is 0.3 mm. If the thickness of the piezoelectric patches is more than 0.3 mm, the largest deflection at the middle of the beam cannot reach 4 cm due to the large rigidity of the beam harvester. The deflection restriction is hence not applicable for those cases, which are not considered in our current studies.

The results of parameter study with different lengths of piezoelectric patches are illustrated in Table 4-3 and Fig. 4-7. The piezoelectric patches are always mounted on the central part of the host beam, where the largest curvature occurs during the vibration close to its first mode with certain excitation frequency (140 rad/s). From Table 4-3 and Fig. 4-7, it is seen that the generated voltage and the output electric power are not linear relative with the increasing percentage of the length of the host beam covered by the piezoelectric patches. This can be interpreted by the coupling effect of the slope difference between the two ends of the piezoelectric patches as well as their capacitance, which are both determined by the length of the patches. With an increment in the length of the piezoelectric patches, although the total charge keeps increasing with larger slope difference between the two ends of the piezoelectric patches from Eq. (2-2), the capacitance of the piezoelectric patches is increased as well resulting in the possible decrease of the voltage and power generation on the piezoelectric patches from Eqs. (2-

3) and (2-19). Therefore, the design with either very short or long length of the piezoelectric patches mounted on the beam harvester is not ideal for an efficient energy harvester. For the proposed beam harvester, while the thickness is fixed (0.3mm), the optimal length of piezoelectric patches is 60% of the length of host beam with the maximum RMS value of power generation of 0.2156 W at the steady state (3s-4s) after tuning.

In addition, the effect of the capacitance of the tuning capacitor and the equivalent electric resistance of the tuning circuit are studied and presented in Fig. 4-8. From Fig. 4-8(a), it is seen that with constant electric resistance (1000Ω), the RMS value of the output electric power increases from 0.0278 W to 0.1387 W, while the capacitance of the tuning capacitor decreases from 500 μF to 10 μF. It also illustrated in Fig. 4-8(b) that with constant capacitance (100 μF), the RMS value of the output electric power increases from 0.0278 W to 0.1387 W, when the equivalent electric resistance decreases from 5000 Ω to 100 Ω. In conclusion, the decreasing of these two variables will speed up the charging of the tuning capacitor, leading to the faster self-tuning process. Thus, the RMS value of the output electric power during the tuning process can be further increased.

4.3 Finite element analysis for verification of self-tuning process

The finite element analysis software ANSYS 17.0 is used to verify the effectiveness of the proposed self-tuning approach. The study of the forced vibration process of the simply supported beam energy harvester is proposed using the transient analysis module provided by ANSYS 17.0.

The finite element model is shown in Fig. 4-9. Normal plane element plane 183 and coupled field element plane 223 are used to mesh the host beam and the piezoelectric patches. Different colors shown in Fig. 4-9 stand for different elements and material properties used for the host beam and piezoelectric patches. The element length of host beam and piezoelectric patches is 1 mm. For the simply supported beam, it is pinned supported at the left end and free to rotate. The y-displacement at the right end is restricted without moment resistance. The host beam structure is assumed to be made of aluminum alloys, hence the voltage of the interfaces between piezoelectric patches and the host beam is set to be zero as the host beam structure is grounded. The piezoelectric patches are poled along the *y* direction shown in Fig. 4-9, therefore, when transverse displacement of the bending beam structure takes place, there will be a voltage output on the top and bottom surfaces of the piezoelectric patches.

The beam harvester is working under a harmonic point load with the excitation frequency is smaller than the first natural frequency of the beam harvester. The tuning process is approached by applying an axial pressure at the right end of the host beam, which is determined by the piezoelectric patches through the charged voltage on the tuning capacitor. The transient analysis module of ANSYS 17.0 is used for the forced vibrational analysis. The transient analysis is separated into 4000 sub-steps during a 1-4 s period with the fixed step length of 0.001s. For each sub-step, the generated voltages from the piezoelectric patches are recorded and used to calculate the charged voltage on the tuning capacitor and the axial pressure applied to the beam structure to realize the frequency tuning of the beam. During the transient analysis process, the axial pressure applied to the beam will keep increasing leading to the decrement of the equivalent stiffness of the beam and increment of the beam deflection until the generated voltage on the piezoelectric patches reaches to certain value corresponding to certain beam deflection

restriction. The tuning process with the increasing voltage generation from FEM analysis will be compared with the tuning process from the theoretical model to verify its effectiveness.

The results from FEM analysis of the self-tuning process are provided in Fig. 4-10 and Fig. 4-11 for a period of 4 seconds. With the same dimensions and material properties listed in Table 4-1, the first natural frequency of the beam harvester is obtained as 151.54 rad/s in modal analysis. The excitation frequency is set to be 140 rad/s in transient analysis. The axial pressure applied on the right end of the beam harvester is decided by the charged voltage on the tuning capacitor, which is calculated from the voltage generation on piezoelectric patches based on Eq. (4-2). To avoid the failure of materials, the beam harvester has the same transverse displacement restriction of 4 cm. Fig. 4-10 illustrates the transverse displacement at the middle of the beam harvester without and with tuning, it is seen that the transverse displacements are 0.8 cm and 4 cm at steady state without and with tuning, respectively. The amplitude of generated voltage after tuning is 45.29 V given in Fig. 4-11, which is 4.86 times of the one (9.31 V) without tuning. Through FEM simulation, the tuning method is proved to be efficient to generate higher output voltage from piezoelectric patches. The deviation of the calculated voltage generation at steady state after tuning between theoretical model and FEM model is 4.6%. Such excellent agreement of the results indicates the effectiveness of the proposed theoretical model and the self-tuning method. In addition, from Fig. 4-10 and Fig. 4-11, it can be seen that the tuning progress along the first 2 seconds in FEM is similar to the one obtained from the theoretical simulation. The vibration amplitude at the middle of the beam without tuning in FEM simulation is a little bit higher than the one from theoretical simulation. This is because of the more rigidity of the Euler-Bernoulli beam model, which is used in theoretical modeling. Convergence study also conducted in FEM simulation on the element size and voltage generation after tuning, which is shown in

Fig. 4-12. It is seen that the element size of 1 mm is small enough giving accurate results of voltage generation.

4.4 Conclusions

In this chapter, the frequency self-tuning is realized by a tuning circuit, a filtering circuit and a piezoelectric stack actuator. Compared to the first tuning method with feedback filtering circuit, the second tuning method provides more stable tuning voltage and feasible controlling technique. Considering the failure of materials due to the large deflection at resonance as well as the over tuning that the natural frequency of the beam harvester passing the excitation frequency, a filtering circuit is designed to automatically cut off the charging of the tuning capacitor when the beam harvester is close to the resonance with the restricted deflection. Through the numerical simulations, the proposed energy harvester can efficiently self-tune its first natural frequency getting close to the excitation frequency within 2 seconds reaching close to the resonant state. The simulation results prove the efficiency of this energy harvesting system, with 26.2 times RMS value of the output electric power comparing to the one without tuning process with the given dimension of the beam harvester (L=0.75m, b=0.02m and h=0.006). Furthermore, parameter studies of the sizes of piezoelectric patches are investigated leading to the optimal length of the piezoelectric patches (60% of the length of the host beam), which increases the RMS value of the power generation by 55% comparing to the one with the preset length (40% of the length of the host beam). It is also noted that smaller capacitance of the tuning capacitor as well as the equivalent electric resistance of the tuning circuit will speed up the tuning process hence result in the further increment of power generation. This research provides an efficient

self-tuning energy harvesting method which does not need external energy input to realize the tuning process.

Table 4-1 Dimensions and material properties of the energy harvesting system.

Parameter	Host beam (aluminum)	Piezoelectric patches	Electric circuit
Young's modulus (N m^{-2})	$E=69\times10^{9}$	$E_p=78\times10^{9}$	-
Mass density (kg m^{-3})	2.8×10^{3}	7.5×10^{3}	-
e_{31} (C m^{-2})	-	-2.8	-
e_{33} (C m^{-2})	-	10	-
d_{31} (C N^{-1})	-	-1.28×10^{-10}	-
C_v (nF)	-	7.5 for a piezoelectric patch with dimensions of 0.02m×0.3m×0.0003m	-
L (m)	0.75	-	-
L_1(m)	0.225	-	-
L_3(m)	0.4	-	
a (m)	-	0.3	-
h (m)	0.006	-	-
h_1 (m)	-	0.0003	-
b (m)	0.02	0.02	-
R (kΩ)	-	-	1
C_o (μF)	-	-	100

Table 4-2 Parameter study with different thickness of piezoelectric patches.

Thickness (mm)	Natural frequency before tuning (rad/s)	Natural frequency after tuning (rad/s)	Maximum charge on piezoelectric patches (C)	Generated voltage from piezoelectric patches (V)	RMS value of output electric power (W)
0.05	151.48	142.03	3.2937e-5	7.32	0.0238
0.1	152.08	141.78	3.3048e-5	14.69	0.0479
0.15	152.63	141.53	3.3111e-5	22.07	0.0722
0.2	153.18	141.28	3.3129e-5	29.41	0.0961
0.25	153.68	140.98	3.3138e-5	36.82	0.1205
0.3	154.10	140.83	3.3150e-5	43.30	0.1389

Table 4-3 Parameter study with different length of piezoelectric patches.

Percentage of length of the host beam (%)	Natural frequency before tuning (rad/s)	Natural frequency after tuning (rad/s)	Maximum charge on piezoelectric patches (C)	Maximum voltage on piezoelectric patches (V)	RMS value of output electric power (W)
20	152.02	141.48	1.5970e-5	42.59	0.0672
30	153.02	141.08	2.4540e-5	42.63	0.1058
40	154.10	140.83	3.3150e-5	43.30	0.1389
50	155.17	140.63	4.0160e-5	42.84	0.1732
60	156.02	140.23	4.7192e-5	41.95	0.2156
70	156.62	140.08	5.2545e-5	40.03	0.2079
80	156.97	140.13	5.6091e-5	37.39	0.2068
90	157.12	140.03	5.8226e-5	34.50	0.1985

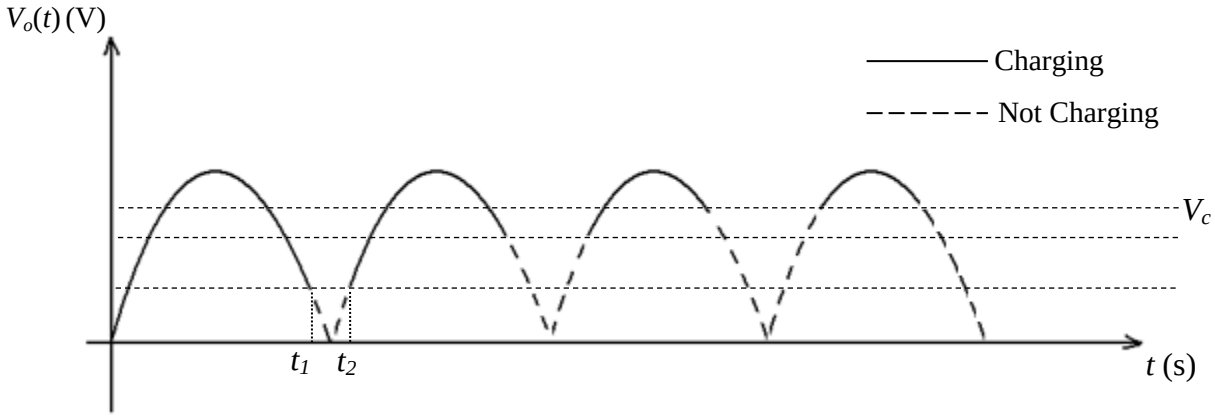
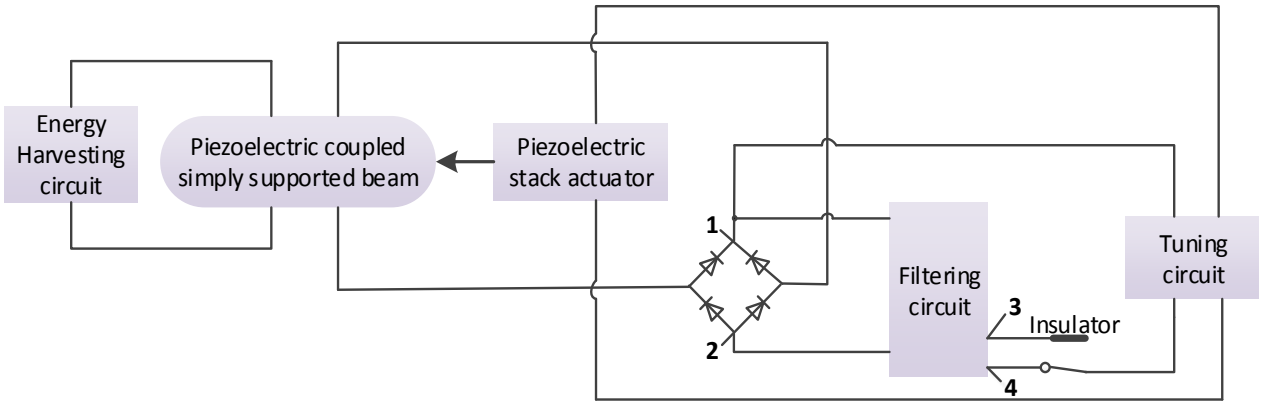
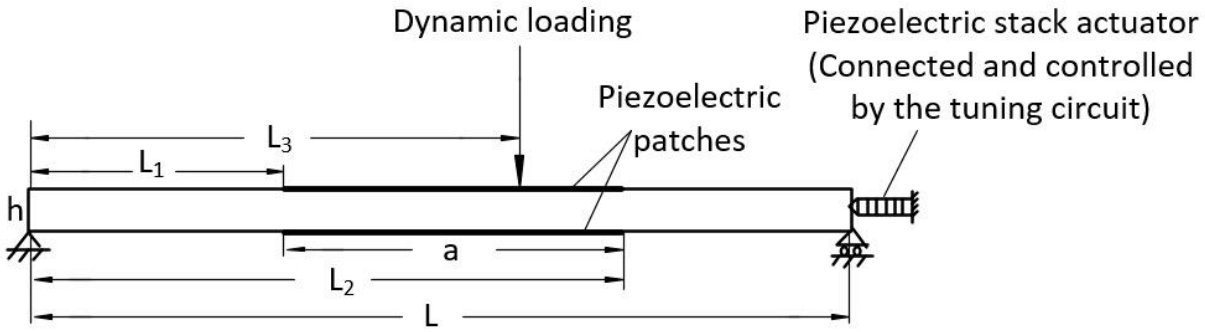


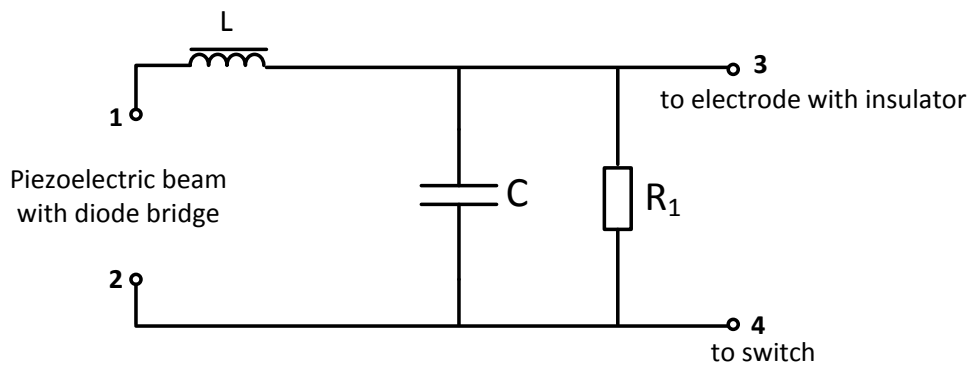
Fig. 4-1 Charging of the tuning capacitor through the diode bridge circuit [31].



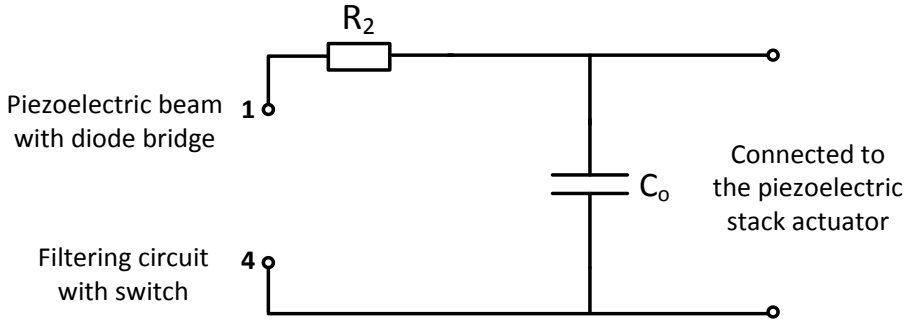
(a) Block diagram of the energy harvesting system



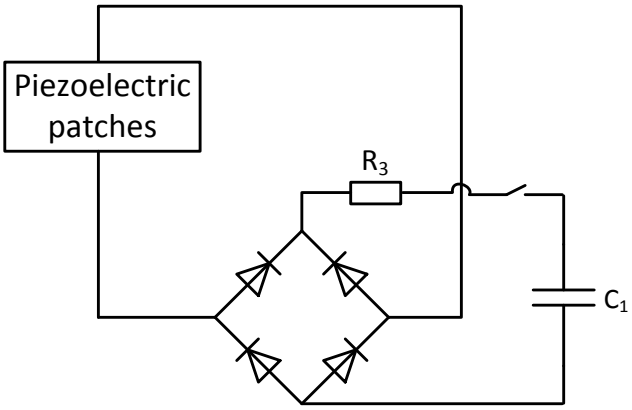
(b) Schematic diagram and geometries of the piezoelectric coupled simply supported beam



(c) Filtering circuit to control the switch



(d) Tuning circuit to control the piezoelectric stack actuator



(e) Energy harvesting circuit

Fig. 4-2 Design of the proposed self-tuning energy harvesting system.

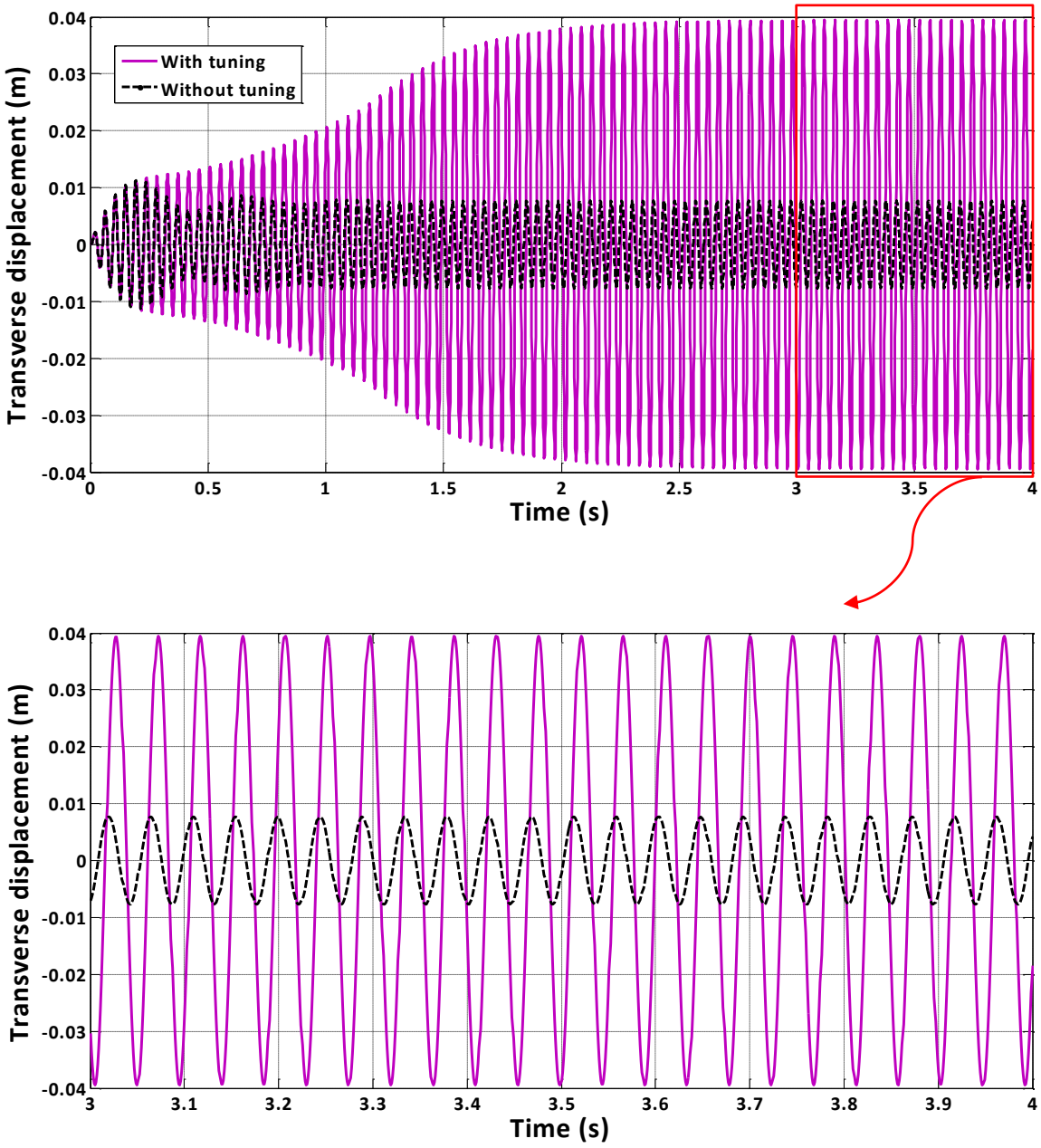
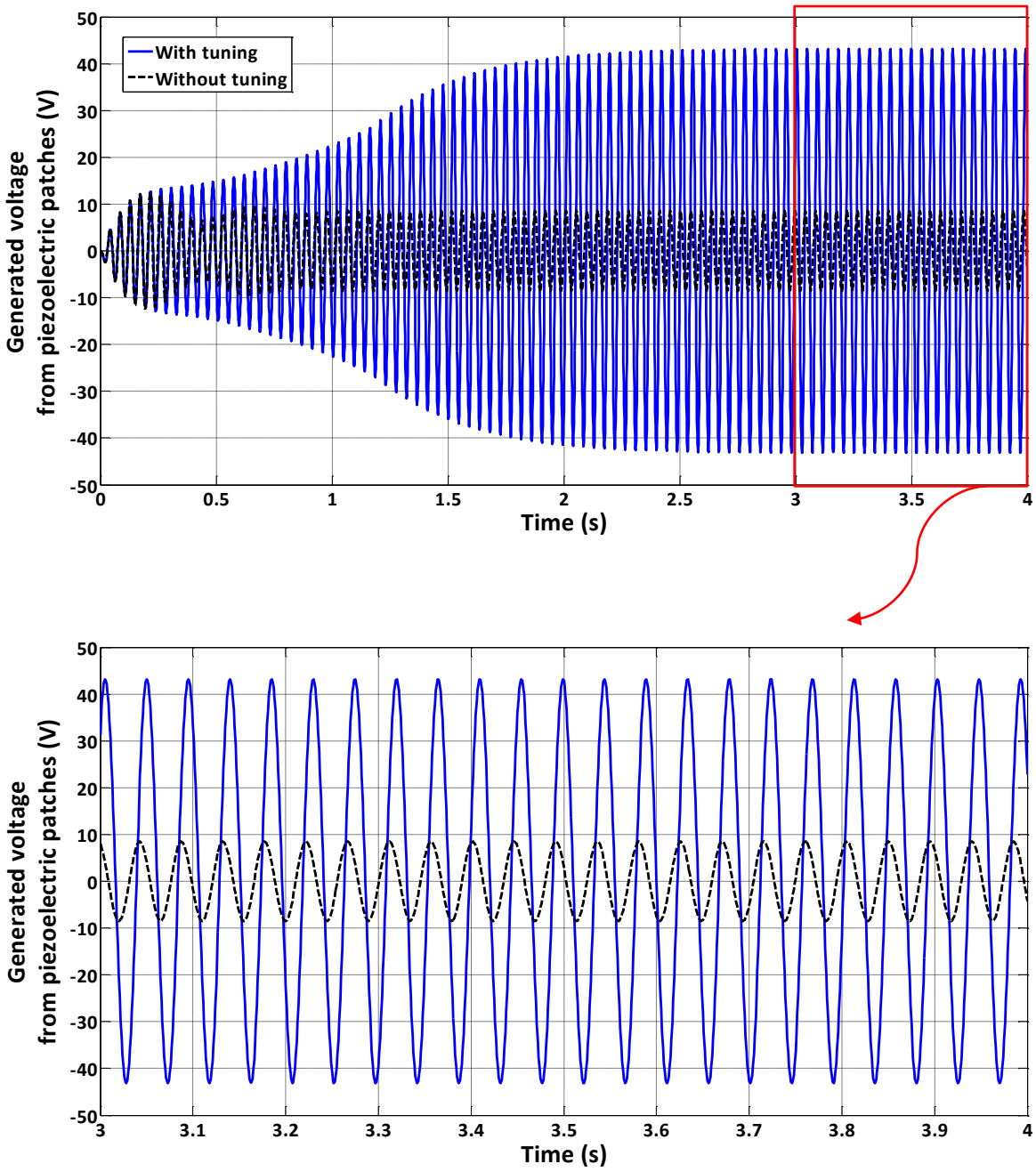
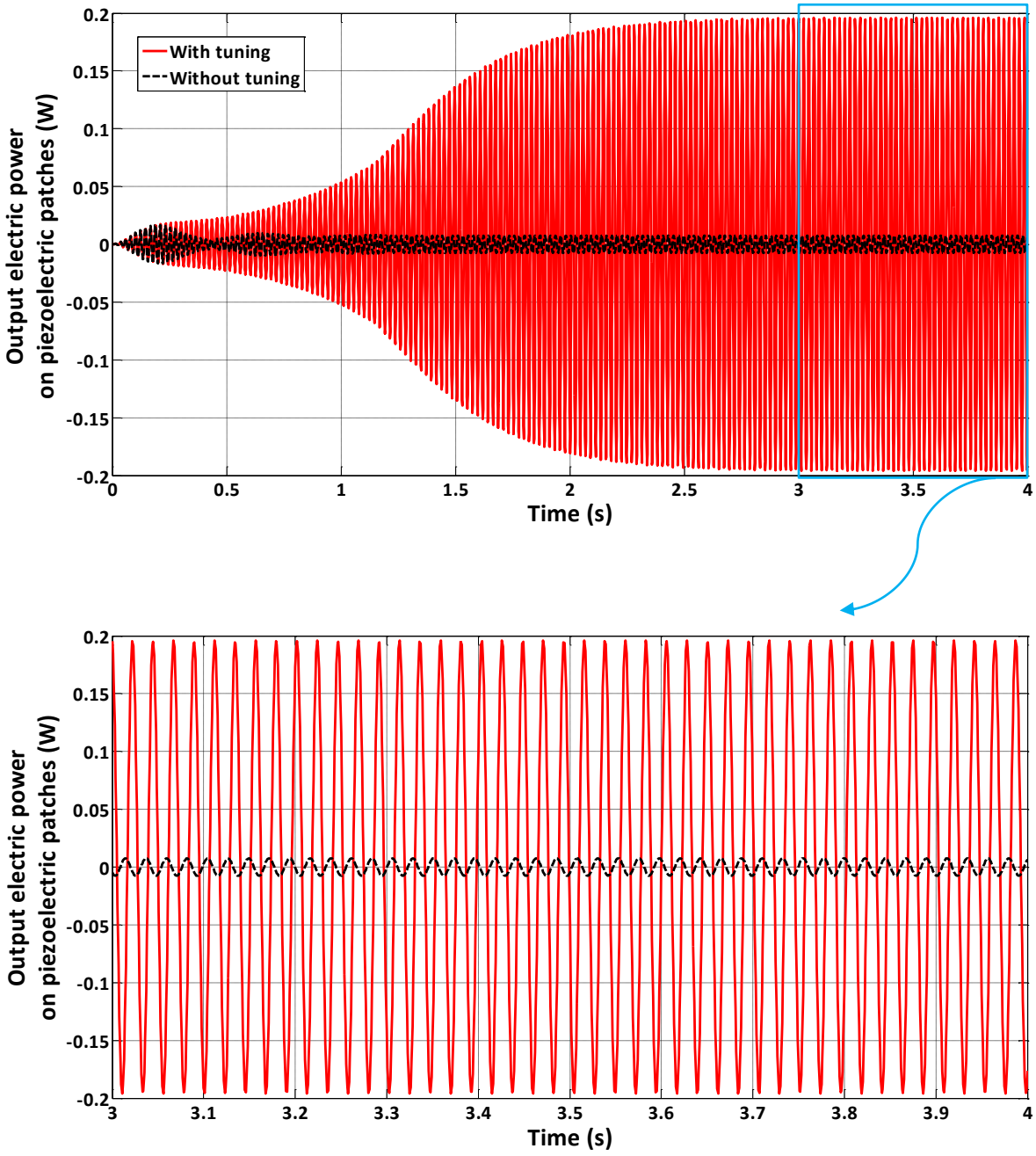


Fig. 4-3 Transverse displacement of the beam harvester with/without tuning.



(a) Generated voltage from the piezoelectric patches



(b) Output electric power on the piezoelectric patches

Fig. 4-4 Voltages and power on piezoelectric patches with/without tuning.

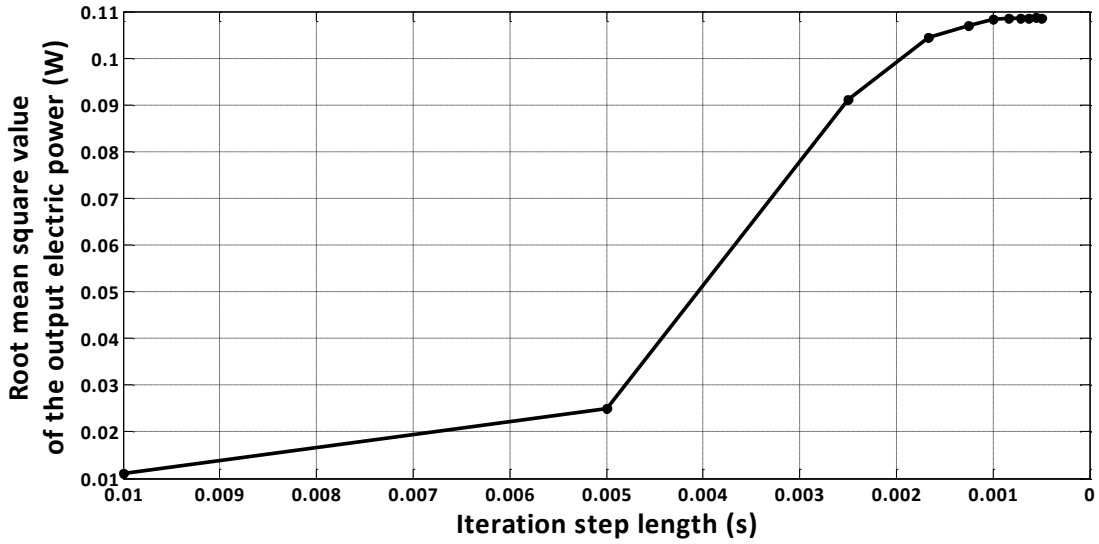


Fig. 4-5 Convergence study of the RMS power output with different iteration step lengths.

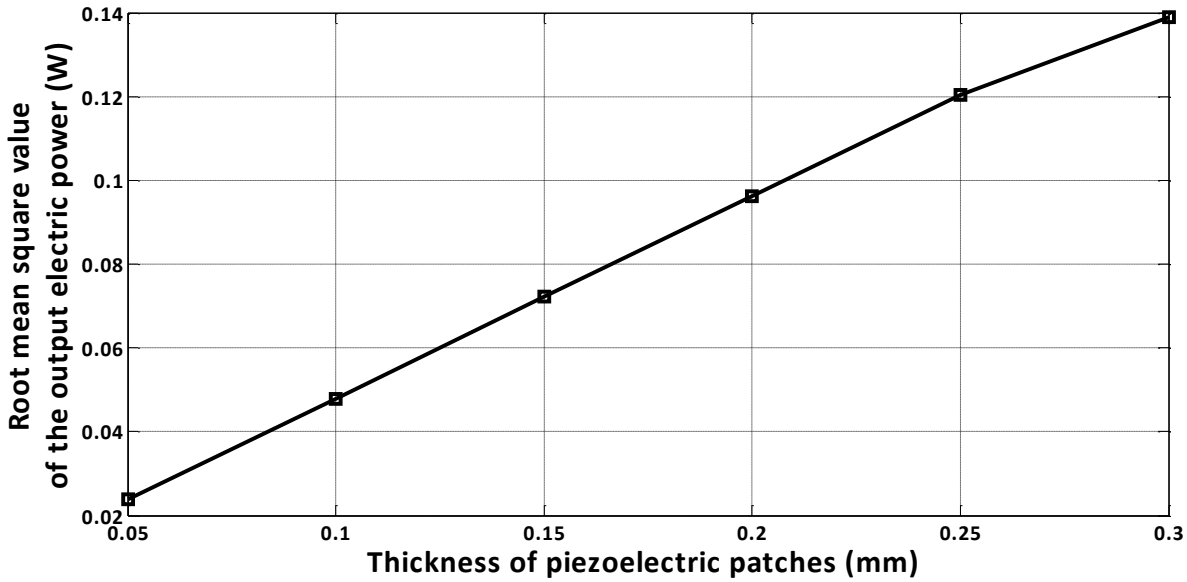
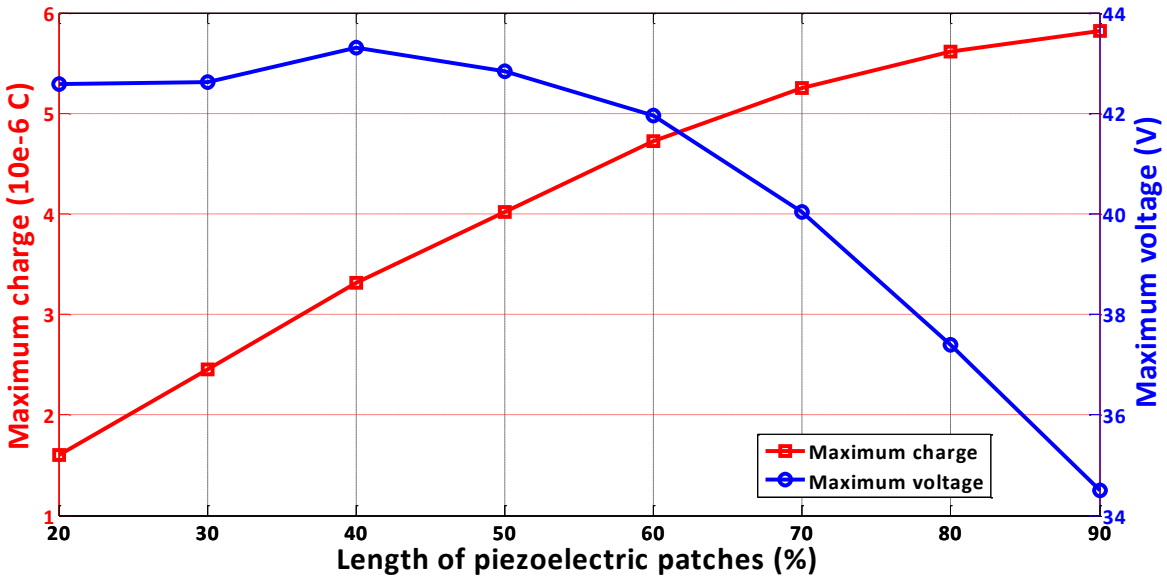
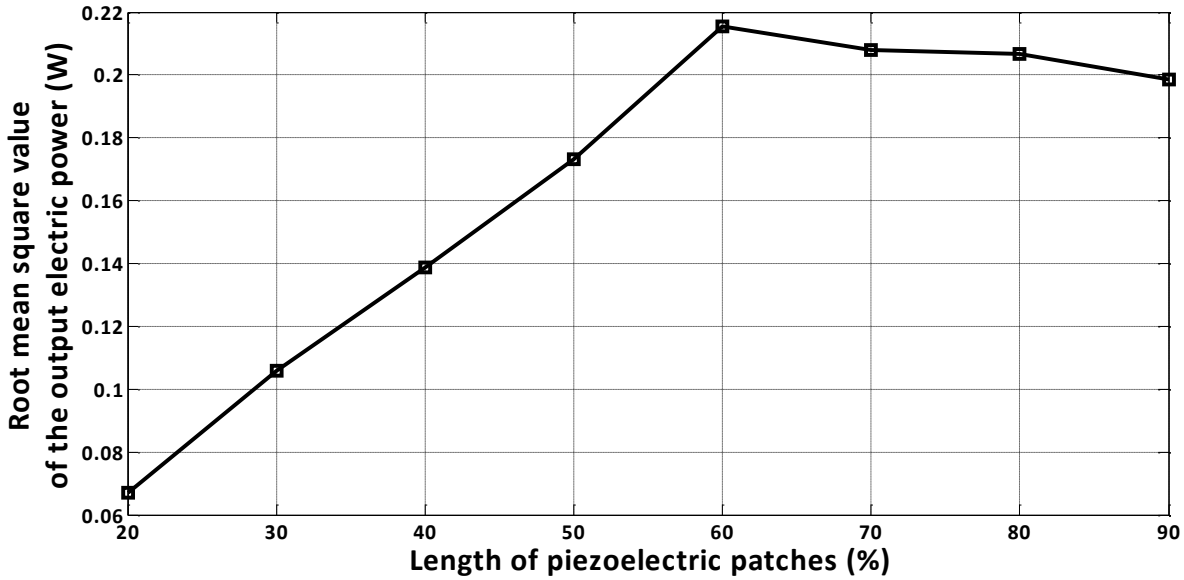


Fig. 4-6 RMS value of the output power versus different thickness of piezoelectric patches.

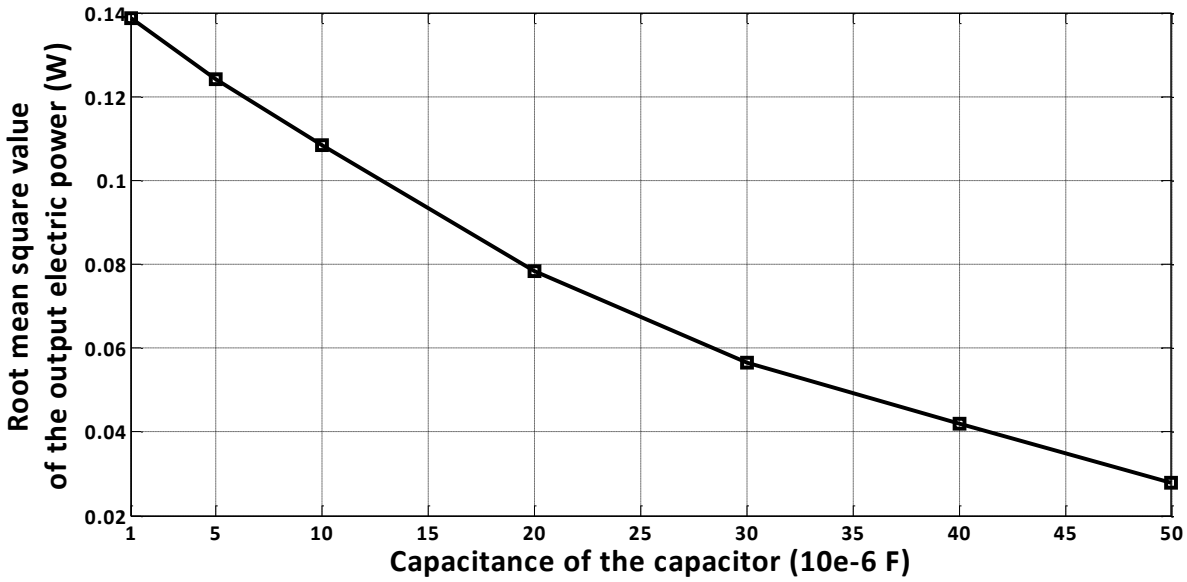


(a) Maximum generated charge and voltage on piezoelectric patches during the tuning process

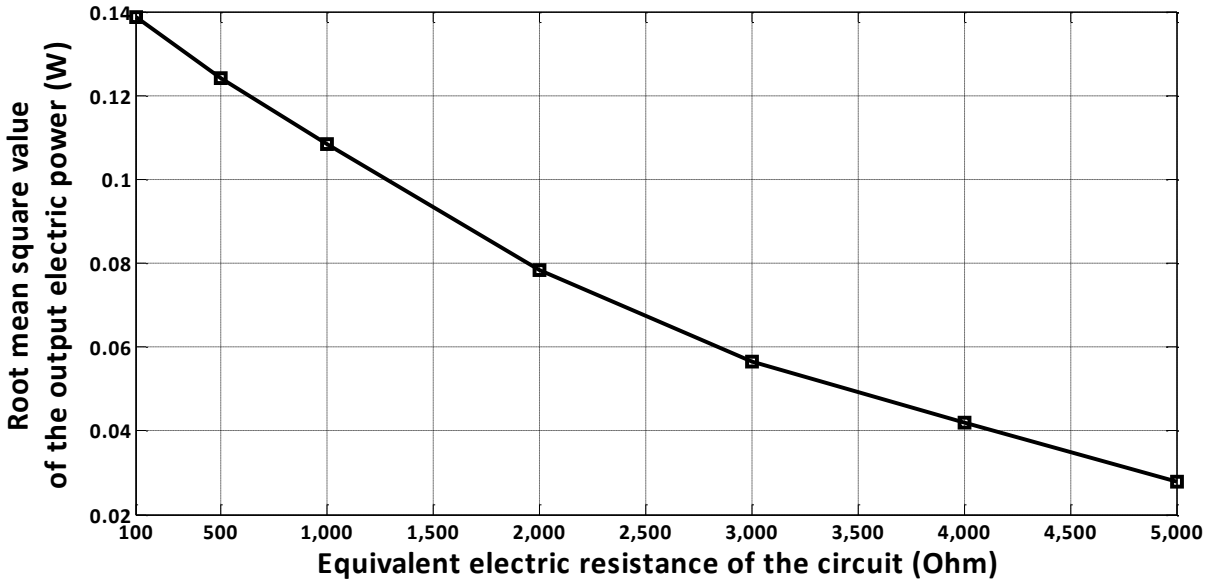


(b) RMS value of the output electric power

Fig. 4-7 Generated charge, voltage and power versus different length of piezoelectric patches.



(a) Different capacitance of the capacitor



(b) Different equivalent electric resistance of the circuit

Fig. 4-8 RMS value of output electric power versus different capacitance and resistance of the tuning circuit.

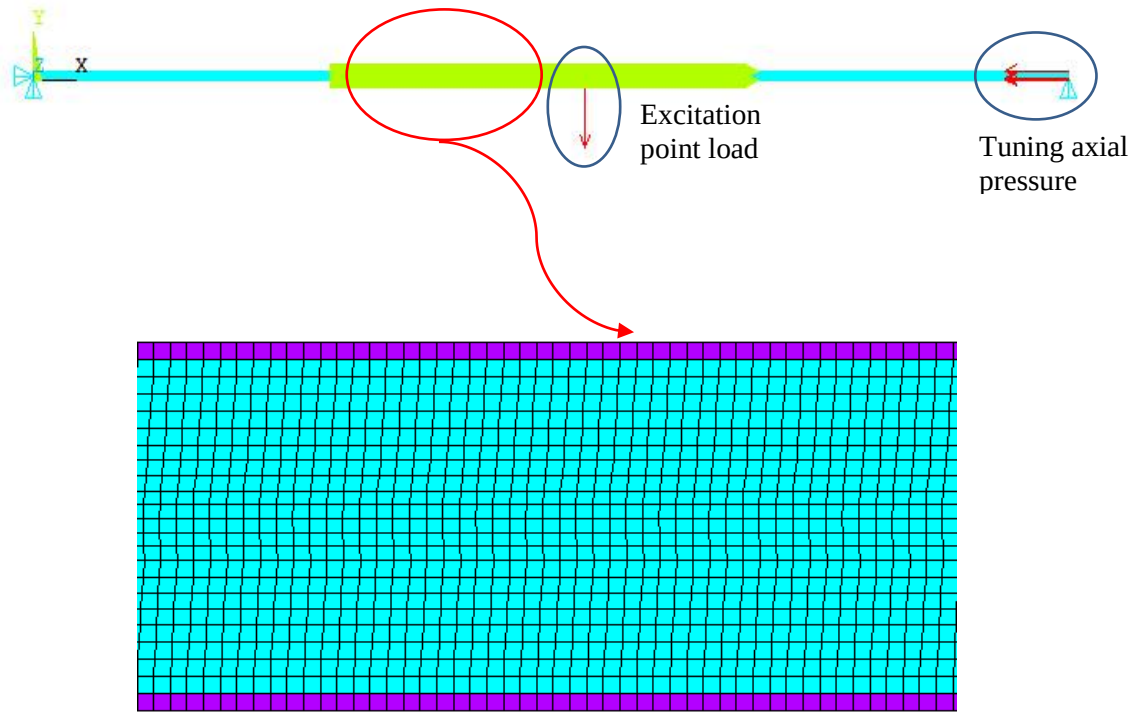
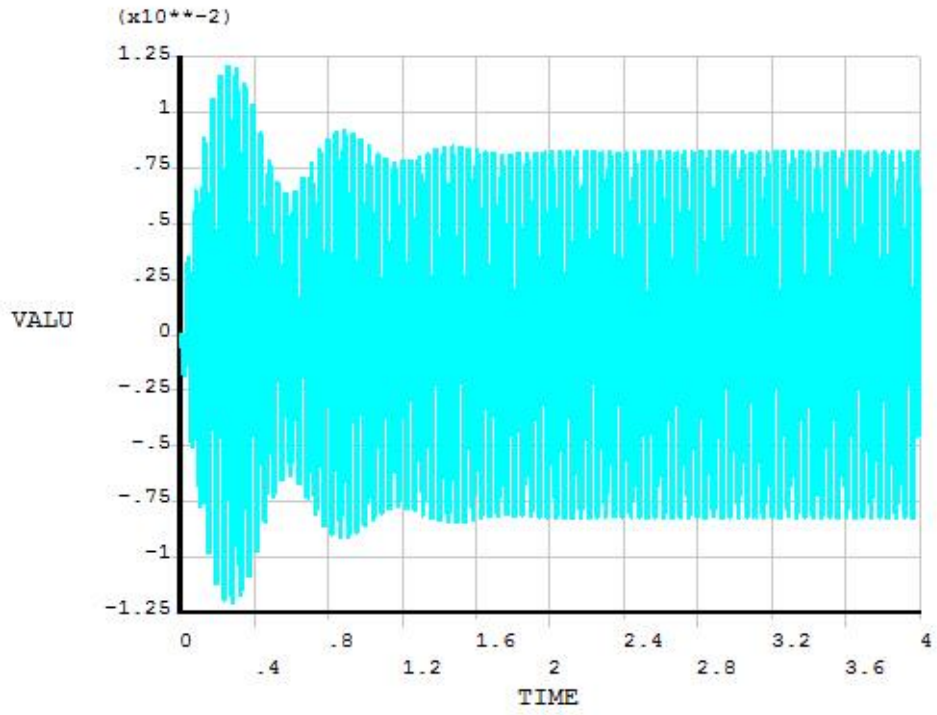
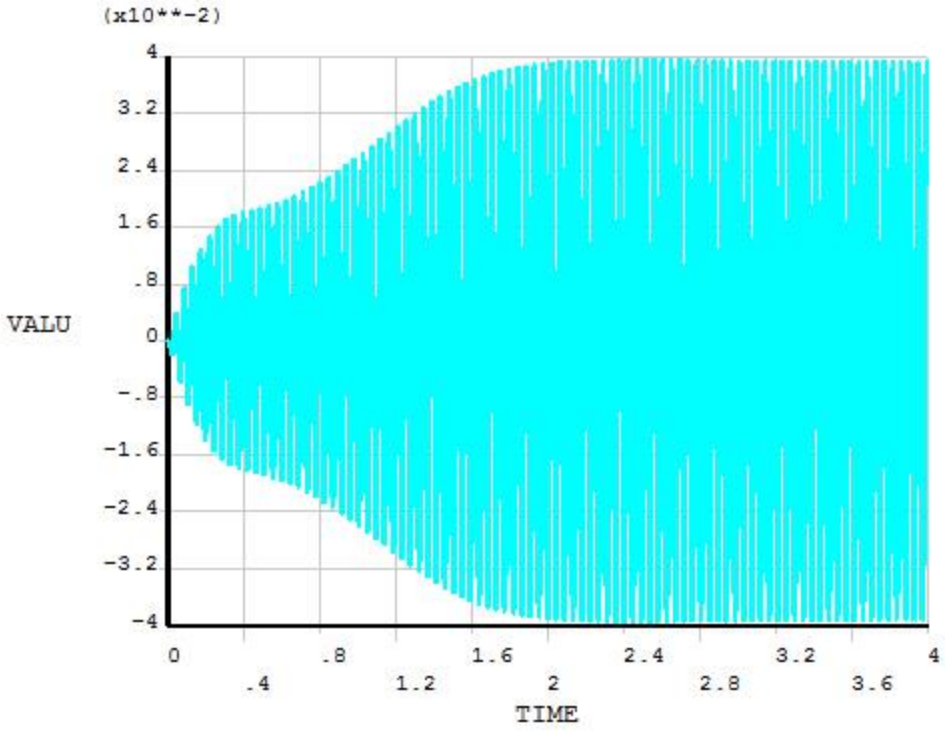


Fig. 4-9 Finite element model of the host beam bonded with piezoelectric patches.



(a)



(b)

Fig. 4-10 Transverse displacement of beam harvester (a) without tuning (b) with tuning.

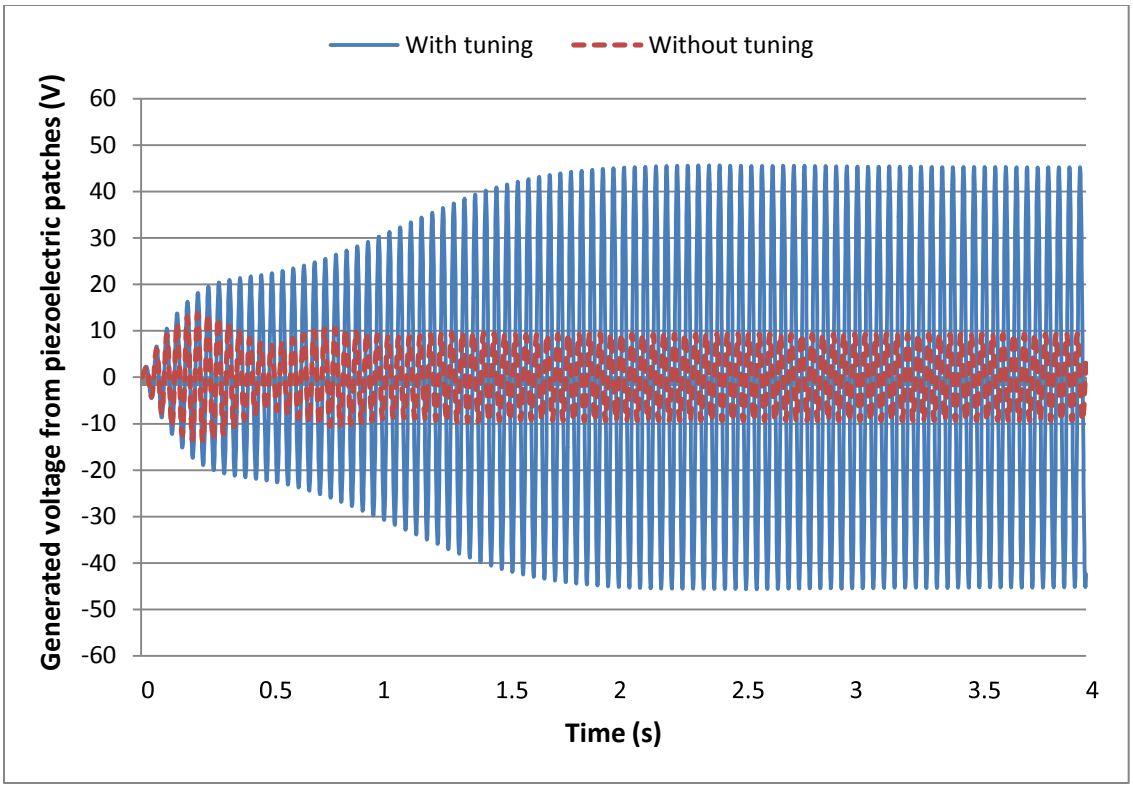


Fig. 4-11 Voltage generation from FEM analysis.

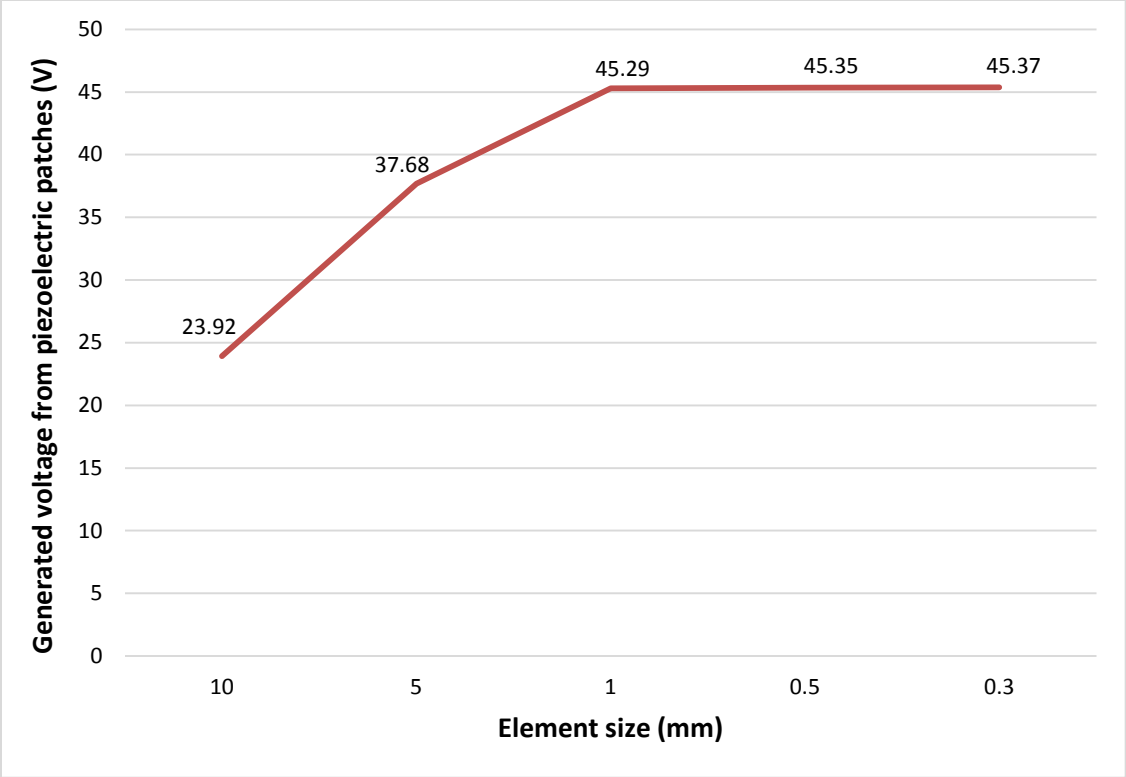


Fig. 4-12 Convergence study of different element size.

5 Conclusions and future work

In this thesis, an efficient self-tuning energy harvesting methodology is proposed and simulated by a simply supported beam model coupled with piezoelectric patches. The frequency self-tuning of the beam harvester is approached through two different electrical circuits. The adjustment of the natural frequency of the beam harvester is implemented by a controlling voltage applied on a piezoelectric stack actuator which generates a compressive axial force. To avoid the failure of materials due to the large deflection near the resonance as well as the over tuning that the natural frequency of the beam harvester passing the excitation frequency, the deflection of the host beam is restricted to 4 cm in all simulations. Through the numerical simulations (both analytical and FEM), following conclusions can be made.

1. The proposed energy harvesting methodology can efficiently self-tune the first natural frequency of the harvester getting close to the excitation frequency reaching to the resonant state with large power generation.

2. The first tuning method with a feedback filtering circuit can realize self-tuning in 0.38s, with 10 times of the power generation compared to the one without tuning. The efficiency of energy harvesting can be further increased with the elongated length of piezoelectric patches to 0.5m.

3. The second tuning method with the combination of a tuning capacitor and a filtering circuit has better tuning effect as more stable tuning voltages are provided to the piezoelectric stack actuator. The higher power generation ratio reaches 26.2 times between the tuned and un-tuned energy harvester.

4. Optimal design of the sizes of piezoelectric patches as well as the components of electric circuits can further improve the RMS value of power generation by more than 55%.

The current research is still at an initial stage, future work can be conducted including experimental verification, development of more efficient self-tuning method which can realize the self-tuning of the energy harvester to match more complicated excitation with randomly changing frequency components.

Bibliography

[1] Ottman GK, Hofmann HF, Bhatt AC, Lesieutre G. Adaptive piezoelectric energy harvesting circuit for wireless remote power supply. Power Electronics, IEEE Transactions on. 2002;17:669-76.
[2] Kansal A, Srivastava MB. An environmental energy harvesting framework for sensor networks. Low Power Electronics and Design, 2003 ISLPED'03 Proceedings of the 2003 International Symposium on: IEEE; 2003. p. 481-6.
[3] Sodano HA, Park G, Inman D. Estimation of electric charge output for piezoelectric energy harvesting. Strain. 2004;40:49-58.
[4] Donelan JM, Li Q, Naing V, Hoffer J, Weber D, Kuo AD. Biomechanical energy harvesting: generating electricity during walking with minimal user effort. Science. 2008;319:807-10.
[5] Mitcheson PD, Miao P, Stark BH, Yeatman E, Holmes A, Green T. MEMS electrostatic micropower generator for low frequency operation. Sensors and Actuators A: Physical. 2004;115:523-9.
[6] Sari I, Balkan T, Kulah H. An electromagnetic micro power generator for wideband environmental vibrations. Sensors and Actuators A: Physical. 2008;145:405-13.
[7] Xie X, Wang Q, Wu N. Energy harvesting from transverse ocean waves by a piezoelectric plate. International Journal of Engineering Science. 2014;81:41-8.
[8] Anton SR, Sodano HA. A review of power harvesting using piezoelectric materials (2003–2006). Smart Materials and Structures. 2007;16:R1.
[9] Priya S. Advances in energy harvesting using low profile piezoelectric transducers. Journal of electroceramics. 2007;19:167-84.
[10] Williams C, Yates RB. Analysis of a micro-electric generator for microsystems. Sensors and Actuators A: Physical. 1996;52:8-11.
[11] Sodano HA, Inman DJ, Park G. Comparison of piezoelectric energy harvesting devices for recharging batteries. Journal of Intelligent Material Systems and Structures. 2005;16:799-807.
[12] Shu Y, Lien I. Analysis of power output for piezoelectric energy harvesting systems. Smart Materials and Structures. 2006;15:1499.
[13] Eichhorn C, Goldschmidtboeing F, Woias P. Bidirectional frequency tuning of a piezoelectric energy converter based on a cantilever beam. Journal of Micromechanics and Microengineering. 2009;19:094006.
[14] Xie X, Wang Q, Wu N. Potential of a piezoelectric energy harvester from sea waves. Journal of Sound and Vibration. 2014;333:1421-9.

[15] Xie X, Wang Q, Wu N. A ring piezoelectric energy harvester excited by magnetic forces. International Journal of Engineering Science. 2014;77:71-8.
[16] Wu N, Wang Q, Xie X. Ocean wave energy harvesting with a piezoelectric coupled buoy structure. Applied Ocean Research. 2015;50:110-8.
[17] Priya S. Modeling of electric energy harvesting using piezoelectric windmill. Applied Physics Letters. 2005;87:184101.
[18] Mateu L, Moll F. Optimum piezoelectric bending beam structures for energy harvesting using shoe inserts. Journal of Intelligent Material Systems and Structures. 2005;16:835-45.
[19] Mateu L, Fonellosa F, Moll F. Electrical characterization of a piezoelectric film-based power generator for autonomous wearable devices. XVIII Conference on Design of Circuits and Integrated Systems. 2003.
[20] Erturk A, Renno JM, Inman DJ. Modeling of piezoelectric energy harvesting from an L-shaped beam-mass structure with an application to UAVs. Journal of Intelligent Material Systems and Structures. 2008.
[21] Xie X, Wu N, Yuen K, Wang Q. Energy harvesting from high-rise buildings by a piezoelectric coupled cantilever with a proof mass. International Journal of Engineering Science. 2013;72:98-106.
[22] Ali SF, Friswell M, Adhikari S. Analysis of energy harvesters for highway bridges. Journal of Intelligent Material Systems and Structures. 2011:1045389X11417650.
[23] Baker J, Roundy S, Wright P. Alternative geometries for increasing power density in vibration energy scavenging for wireless sensor networks. Proc 3rd Int Energy Conversion Engineering Conf(San Francisco, CA, Aug)2005. p. 959-70.
[24] Roundy S, Wright PK, Rabaey J. A study of low level vibrations as a power source for wireless sensor nodes. Computer communications. 2003;26:1131-44.
[25] Yang J, Zhou H, Hu Y, Jiang Q. Performance of a piezoelectric harvester in thickness-stretch mode of a plate. ieee transactions on ultrasonics, ferroelectrics, and frequency control. 2005;52:1872-6.
[26] Zhu D, Tudor MJ, Beeby SP. Strategies for increasing the operating frequency range of vibration energy harvesters: a review. Measurement Science and Technology. 2010;21:022001.
[27] Mann B, Sims N. Energy harvesting from the nonlinear oscillations of magnetic levitation. Journal of Sound and Vibration. 2009;319:515-30.
[28] Cornwell P, Goethal J, Kowko J, Damianakis M. Enhancing power harvesting using a tuned auxiliary structure. Journal of Intelligent Material Systems and Structures. 2005;16:825-34.
[29] Xue H, Hu Y, Wang Q-M. Broadband piezoelectric energy harvesting devices using multiple bimorphs with different operating frequencies. Ultrasonics, Ferroelectrics, and Frequency Control, IEEE Transactions on. 2008;55:2104-8.
[30] Sari I, Balkan T, Kulah H. A wideband electromagnetic micro power generator for wireless microsystems. TRANSDUCERS 2007-2007 International Solid-State Sensors, Actuators and Microsystems Conference: IEEE; 2007. p. 275-8.

[31] Wang Q, Wu N. Optimal design of a piezoelectric coupled beam for power harvesting. Smart Materials and Structures. 2012;21:085013.
[32] Wu N, Wang Q, Xie X. Wind energy harvesting with a piezoelectric harvester. Smart Materials and Structures. 2013;22:095023.
[33] Challa VR, Prasad M, Shi Y, Fisher FT. A vibration energy harvesting device with bidirectional resonance frequency tunability. Smart Materials and Structures. 2008;17:015035.
[34] Challa VR, Prasad M, Fisher FT. Towards an autonomous self-tuning vibration energy harvesting device for wireless sensor network applications. Smart Materials and Structures. 2011;20:025004.
[35] Aboulfotoh NA, Arafa MH, Megahed SM. A self-tuning resonator for vibration energy harvesting. Sensors and Actuators A: Physical. 2013;201:328-34.
[36] Wu X, Lin J, Kato S, Zhang K, Ren T, Liu L. A frequency adjustable vibration energy harvester. Proceedings of PowerMEMS. 2008:245-8.
[37] Scheibner D, Mehner J, Reuter D, Kotarsky U, Gessner T, Dötzel W. Characterization and self-test of electrostatically tunable resonators for frequency selective vibration measurements. Sensors and Actuators A: Physical. 2004;111:93-9.
[38] Scheibner D, Mehner J, Reuter D, Gessner T, Dötzel W. A spectral vibration detection system based on tunable micromechanical resonators. Sensors and Actuators A: Physical. 2005;123:63-72.
[39] Lee KB, Lin L, Cho Y-H. A closed-form approach for frequency tunable comb resonators with curved finger contour. Sensors and Actuators A: Physical. 2008;141:523-9.
[40] Peters C, Maurath D, Schock W, Manoli Y. Novel electrically tunable mechanical resonator for energy harvesting. Proceedings PowerMEMS 2008. 2008:253-6.
[41] Wu W-J, Chen Y-Y, Lee B-S, He J-J, Peng Y-T. Tunable resonant frequency power harvesting devices. Smart Structures and Materials: International Society for Optics and Photonics; 2006. p. 61690A-A-8.
[42] Roundy S, Zhang Y. Toward self-tuning adaptive vibration-based microgenerators. Smart Materials, Nano-, and Micro-Smart Systems: International Society for Optics and Photonics; 2005. p. 373-84.
[43] Hoffmann D, Willmann A, Hehn T, Folkmer B, Manoli Y. A self-adaptive energy harvesting system. Smart Materials and Structures. 2016;25:035013.
[44] Lallart M, Anton SR, Inman DJ. Frequency self-tuning scheme for broadband vibration energy harvesting. Journal of Intelligent Material Systems and Structures. 2010.
[45] Eichhorn C, Tchagsim R, Wilhelm N, Woias P. A smart and self-sufficient frequency tunable vibration energy harvester. Journal of Micromechanics and Microengineering. 2011;21:104003.
[46] Gu L, Livermore C. Passive self-tuning energy harvester for extracting energy from rotational motion. Applied Physics Letters. 2010;97:081904.
[47] Gu L, Livermore C. Compact passively self-tuning energy harvesting for rotating applications. Smart Materials and Structures. 2012;21:015002.

[48] Bokaian A. Natural frequencies of beams under compressive axial loads. Journal of Sound and Vibration. 1988;126:49-65.
[49] Cabuz C, Fukatsu K, Hashimoto H, Shoji S, Kurabayashi T, Minami K, et al. Fine frequency tuning in resonant sensors. Micro Electro Mechanical Systems, 1994, MEMS'94, Proceedings, IEEE Workshop on: IEEE; 1994. p. 245-50.
[50] Hu Y, Xue H, Hu H. A piezoelectric power harvester with adjustable frequency through axial preloads. Smart Materials and Structures. 2007;16:1961.
[51] Leland ES, Wright PK. Resonance tuning of piezoelectric vibration energy scavenging generators using compressive axial preload. Smart Materials and Structures. 2006;15:1413.
[52] Lee C-K, Moon FC. Modal sensors/actuators. Journal of applied mechanics. 1990;57:434-41.
[53] Lin C-C, Hsu C-Y. Static shape control of smart beam plates laminated with sine sensors and actuators. Smart Materials and Structures. 1999;8:519.
[54] Sun D, Wang D, Xu Z, Wu H. Distributed piezoelectric element method for vibration control of smart plates. AIAA journal. 1999;37:1459-63.
[55] Crawley EF, De Luis J. Use of piezoelectric actuators as elements of intelligent structures. AIAA journal. 1987;25:1373-85.
[56] Wu N. Study of forced vibration response of a beam with a breathing crack using iteration method. Journal of Mechanical Science and Technology. 2015;29:2827-35.
[57] Cheng Y, Wu N, Zhao S. Study on High Efficiency Energy Harvesting Using Piezoelectric Coupled Beam With Self-Tuning Process. ASME 2015 International Mechanical Engineering Congress and Exposition: American Society of Mechanical Engineers; 2015. p. V04BTA047-V04BT04A.
[58] Mott RL, Cabaj M. Machine elements in mechanical design. 2014.

Appendix A: Matlab code for numerical simulations

The matlab code to realize the numerial simulation process during the study is listed below as reference. All variables are left as blank. With different dimension, material properties and parameters of the harvester, actuator and tuning cirtuits, the tuning process and electrical output will vary.

```
% Efficient piezoelectric energy harvesting with frequency self-tuning
% Yukun Cheng

%============ variable definition ============
% define the structure dimensions (meters)
L; a; L1; L2; h; h1; b;
Ah; % thickness of stack actuator, along the beam axial direction
D; % damping ratio
pf; % Location of the point force (external excitation)

% materials properties
E; Ep; % Young's modulus
Y=E*h/(Ep*h1);
I=b*h^3/12;
p; p1; % Density
A=E*I+Ep*b*((h+2*h1)^3-h^3)/12; % E*I of the second part
pA=p*b*h+2*p1*b*h1; % mass of the second part

Cvo; % Capacitance of the capacitor
R; % equivalent electric resistance of the circuit
e31; e33; d31;
Cv;
Cvv=Cv/b; % the electric capacity per unit width of the piezo layer

% external excitation (point load)
w1;

tx; % Step length
TD; % Time Duration
for t=tx:tx:TD
   t1=t-tx;
   t2=t;
   Tim(tn)=t;

if RE==1;

%============ calculate the natural frequency ============
i=1; j=1;
```

```
for w=0:0.05:2000

    k1=(((P/(2*E*I))^2+p*h*b*w^2/(E*I))^0.5-P/(2*E*I))^0.5;
    k2=(((P/(2*E*I))^2+p*h*b*w^2/(E*I))^0.5+P/(2*E*I))^0.5;
    k3=(((P/(2*A))^2+pA*w^2/A)^0.5-P/(2*A))^0.5;
    k4=(((P/(2*A))^2+pA*w^2/A)^0.5+P/(2*A))^0.5;

    T=-r*E*h^2*(h+h1)*b*d31*(-e31)/(4*h1*(Y+6));

        M=[0,1,0,1,0,0,0,0,0,0,0,0,0,0,0,0;...%1

        0,k1^2,0,-k2^2,0,0,0,0,0,0,0,0,0,0,0,0;...%2

        sinh(k1*L1),cosh(k1*L1),sin(k2*L1),cos(k2*L1),-sinh(k3*L1),-cosh(k3*L1),-sin(k4*L1),-
cos(k4*L1),0,0,0,0,0,0,0,0;...%3

        cosh(k1*L1)*k1,sinh(k1*L1)*k1,cos(k2*L1)*k2,-sin(k2*L1)*k2,-cosh(k3*L1)*k3,-sinh(k3*L1)*k3,-
cos(k4*L1)*k4,sin(k4*L1)*k4,0,0,0,0,0,0,0,0;...%4

    E*I*cosh(k1*L1)*k1^3,E*I*sinh(k1*L1)*k1^3,-E*I*cos(k2*L1)*k2^3,E*I*sin(k2*L1)*k2^3,...
        -A*cosh(k3*L1)*k3^3,-A*sinh(k3*L1)*k3^3,A*cos(k4*L1)*k4^3,-A*sin(k4*L1)*k4^3,0,0,0,0,0,0,0,0;...%5

    I*E*sinh(k1*L1)*k1^2,I*E*cosh(k1*L1)*k1^2,-I*E*sin(k2*L1)*k2^2,-I*E*cos(k2*L1)*k2^2,-
A*sinh(k3*L1)*k3^2+T*cosh(k3*(L1-0))*k3,...
    -A*cosh(k3*L1)*k3^2+T*sinh(k3*(L1-0))*k3,A*sin(k4*L1)*k4^2+T*cos(k4*(L1-0))*k4,...
    A*cos(k4*L1)*k4^2-T*sin(k4*(L1-0))*k4,-T*cosh(k3*(L1+a+0))*k3,-T*sinh(k3*(L1+a+0))*k3,-
T*cos(k4*(L1+a+0))*k4,...
    T*sin(k4*(L1+a+0))*k4,0,0,0,0;...%6

    0,0,0,0,sinh(k3*(L1+a/2)),cosh(k3*(L1+a/2)),sin(k4*(L1+a/2)),cos(k4*(L1+a/2)),-sinh(k3*(L1+a/2)),-
cosh(k3*(L1+a/2)),-sin(k4*(L1+a/2)),-cos(k4*(L1+a/2)),0,0,0,0;...%7

0,0,0,0,cosh(k3*(L1+a/2))*k3+U*L*sinh(k3*(L1+a/2))*k3^2,sinh(k3*(L1+a/2))*k3+U*L*cosh(k3*(L1+a/2))*k3^
2,cos(k4*(L1+a/2))*k4-U*L*sin(k4*(L1+a/2))*k4^2,...
    -sin(k4*(L1+a/2))*k4-U*L*cos(k4*(L1+a/2))*k4^2,-cosh(k3*(L1+a/2))*k3,-sinh(k3*(L1+a/2))*k3,-
cos(k4*(L1+a/2))*k4,sin(k4*(L1+a/2))*k4,0,0,0,0;...%8

    0,0,0,0,sinh(k3*(L1+a/2))*k3^2,cosh(k3*(L1+a/2))*k3^2,-sin(k4*(L1+a/2))*k4^2,-cos(k4*(L1+a/2))*k4^2,...
        -sinh(k3*(L1+a/2))*k3^2,-
cosh(k3*(L1+a/2))*k3^2,sin(k4*(L1+a/2))*k4^2,cos(k4*(L1+a/2))*k4^2,0,0,0,0;...%9

    0,0,0,0,cosh(k3*(L1+a/2))*k3^3,sinh(k3*(L1+a/2))*k3^3,-cos(k4*(L1+a/2))*k4^3,sin(k4*(L1+a/2))*k4^3,...
    -cosh(k3*(L1+a/2))*k3^3,-sinh(k3*(L1+a/2))*k3^3,cos(k4*(L1+a/2))*k4^3,-
sin(k4*(L1+a/2))*k4^3,0,0,0,0;...%10

    0,0,0,0,0,0,0,0,sinh(k3*(L1+a)),cosh(k3*(L1+a)),sin(k4*(L1+a)),cos(k4*(L1+a)),-sinh(k1*(L1+a)),-
cosh(k1*(L1+a)),-sin(k2*(L1+a)),-cos(k2*(L1+a));...%11

    0,0,0,0,0,0,0,0,cosh(k3*(L1+a))*k3,sinh(k3*(L1+a))*k3,cos(k4*(L1+a))*k4,-sin(k4*(L1+a))*k4,...
        -cosh(k1*(L1+a))*k1,-sinh(k1*(L1+a))*k1,-cos(k2*(L1+a))*k2,sin(k2*(L1+a))*k2;...%12

    0,0,0,0,T*cosh(k3*(L1-0))*k3,T*sinh(k3*(L1-0))*k3,T*cos(k4*(L1-0))*k4,-T*sin(k4*(L1-0))*k4,...
```

```
   -A*sinh(k3*(L1+a))*k3^2-T*cosh(k3*(L1+a+0))*k3,-A*cosh(k3*(L1+a))*k3^2-
T*sinh(k3*(L1+a+0))*k3,A*sin(k4*(L1+a))*k4^2-T*cos(k4*(L1+a+0))*k4,...
A*cos(k4*(L1+a))*k4^2+T*sin(k4*(L1+a+0))*k4,E*I*sinh(k1*(L1+a))*k1^2,E*I*cosh(k1*(L1+a))*k1^2,-
E*I*sin(k2*(L1+a))*k2^2,-E*I*cos(k2*(L1+a))*k2^2;...%13

   0,0,0,0,0,0,0,0,A*cosh(k3*(L1+a))*k3^3,A*sinh(k3*(L1+a))*k3^3,-
A*cos(k4*(L1+a))*k4^3,A*sin(k4*(L1+a))*k4^3,...
       -E*I*cosh(k1*(L1+a))*k1^3,-E*I*sinh(k1*(L1+a))*k1^3,E*I*cos(k2*(L1+a))*k2^3,-
E*I*sin(k2*(L1+a))*k2^3;...%14

       0,0,0,0,0,0,0,0,0,0,0,0,sinh(k1*L),cosh(k1*L),sin(k2*L),cos(k2*L);...%15

   0,0,0,0,0,0,0,0,0,0,0,0,sinh(k1*L)*k1^2,cosh(k1*L)*k1^2,-sin(k2*L)*k2^2,-cos(k2*L)*k2^2];%16

     x(i)=w;
   dm(i)=det(M);
   if ((i>=2) && ((dm(i-1)*dm(i))<0))
      f(j)=(x(i-1)+x(i))/2;
      j=j+1;
   end
   i=i+1;
end

%============ Mode Shapes ============

for n=1:3
   w=f(n);

   M2=M(1:15,1:15);
   MI2=inv(M2);
   cc=-MI2*M(1:15,16);
   c1=double(cc(1)); c2=double(cc(2)); c3=double(cc(3)); c4=double(cc(4));
   c5=double(cc(5)); c6=double(cc(6)); c7=double(cc(7)); c8=double(cc(8));
   c9=double(cc(9)); c10=double(cc(10));
   c11=double(cc(11)); c12=double(cc(12));
   c13=double(cc(13)); c14=double(cc(14)); c15=double(cc(15)); c16=1;

   i=1;
   dx=0.001;
   W11=0;
   W12=0;
   for x=0:dx:L1-dx
      xx(i)=x;
      S(i,n)=c1*sinh(k1*x)+c2*cosh(k1*x)+c3*sin(k2*x)+c4*cos(k2*x);
      W11=W11+S(i,n)*dx;
      W12=W12+S(i,n).*S(i,n)*dx;
      i=i+1;
   end
   Mark1=i;
   bn1=p*b*h*W12;
   cn1=w1^2*p*b*h*W11;

   W21=0;
   W22=0;
```

```
    for x=L1:dx:L1+a/2-dx
        xx(i)=x;
        S(i,n)=c5*sinh(k3*x)+c6*cosh(k3*x)+c7*sin(k4*x)+c8*cos(k4*x);
        W21=W21+S(i,n)*dx;
        W22=W22+S(i,n).*S(i,n)*dx;
        i=i+1;
    end

    for x=L1+a/2:dx:L1+a-dx
        xx(i)=x;
        S(i,n)=c9*sinh(k3*x)+c10*cosh(k3*x)+c11*sin(k4*x)+c12*cos(k4*x);
        W21=W21+S(i,n)*dx;
        W22=W22+S(i,n).*S(i,n)*dx;
        i=i+1;
    end
    Mark2=i;
    bn2=pA*W22;
    cn2=w1^2*pA*W21;

    W31=0;
    W32=0;
    for x=L1+a:dx:L
        xx(i)=x;
        S(i,n)=c13*sinh(k1*x)+c14*cosh(k1*x)+c15*sin(k2*x)+c16*cos(k2*x);
        W31=W31+S(i,n)*dx;
        W32=W32+S(i,n).*S(i,n)*dx;
        i=i+1;
    end
    bn3=p*b*h*W32;
    cn3=w1^2*p*b*h*W31;

    Bn(n)=bn1+bn2+bn3;
    Cn(n)=f0*S(pf/dx,n);

end

end

for n=1:3

    w=f(n); % natural frequency
    wd=f(n)*sqrt(1-D^2); % damped frequency

BB(n)=(qndt1(n)*exp(D*w*t1)+D*w*qn1(n)*exp(D*w*t1)+qn1(n)*exp(D*w*t1)*wd*sin(wd*t1)/cos(wd*t1))/(wd
*(sin(wd*t1))^2/cos(wd*t1)+wd*cos(wd*t1));

AA(n)=(qn1(n)*exp(D*w*t1)-BB(n)*sin(wd*t1))/cos(wd*t1);

qq=D^3*cos(t*wd+t1*w1-t1*wd)*exp(-D*t*w+D*t1*w)*w^3-D^3*cos(t*wd-t1*w1-t1*wd)*exp(-
D*t*w+D*t1*w)*w^3+D^2*sin(t*wd+t1*w1-t1*wd)*exp(-D*t*w+D*t1*w)*w^2*w1-D^2*sin(t*wd+t1*w1-
t1*wd)*exp(-D*t*w+D*t1*w)*w^2*wd+D^2*sin(t*wd-t1*w1-t1*wd)*exp(-
D*t*w+D*t1*w)*w^2*w1+D^2*sin(t*wd-t1*w1-t1*wd)*exp(-
D*t*w+D*t1*w)*w^2*wd+2*D^2*sin(w1*t)*w^2*wd+D*cos(t*wd+t1*w1-t1*wd)*exp(-
D*t*w+D*t1*w)*w*w1^2+2*D*cos(t*wd+t1*w1-t1*wd)*exp(-D*t*w+D*t1*w)*w*w1*wd+D*cos(t*wd+t1*w1-
```

```
t1*wd)*exp(-D*t*w+D*t1*w)*w*wd^2-D*cos(t*wd-t1*w1-t1*wd)*exp(-
D*t*w+D*t1*w)*w*w1^2+2*D*cos(t*wd-t1*w1-t1*wd)*exp(-D*t*w+D*t1*w)*w*w1*wd-D*cos(t*wd-t1*w1-
t1*wd)*exp(-D*t*w+D*t1*w)*w*wd^2-4*D*cos(w1*t)*w*w1*wd+sin(t*wd+t1*w1-t1*wd)*exp(-
D*t*w+D*t1*w)*w1^3+sin(t*wd+t1*w1-t1*wd)*exp(-D*t*w+D*t1*w)*w1^2*wd-sin(t*wd+t1*w1-t1*wd)*exp(-
D*t*w+D*t1*w)*w1*wd^2-sin(t*wd+t1*w1-t1*wd)*exp(-D*t*w+D*t1*w)*wd^3+sin(t*wd-t1*w1-t1*wd)*exp(-
D*t*w+D*t1*w)*w1^3-sin(t*wd-t1*w1-t1*wd)*exp(-D*t*w+D*t1*w)*w1^2*wd-sin(t*wd-t1*w1-t1*wd)*exp(-
D*t*w+D*t1*w)*w1*wd^2+sin(t*wd-t1*w1-t1*wd)*exp(-D*t*w+D*t1*w)*wd^3-
2*sin(w1*t)*w1^2*wd+2*sin(w1*t)*wd^3;
   qq1=(D^2*w^2+w1^2-2*w1*wd+wd^2)*(D^2*w^2+w1^2+2*w1*wd+wd^2);
   qqq=-D*sin(t*wd+t1*w1-t1*wd)*wd^2*exp(-D*t*w+D*t1*w)*w*w1+2*D*sin(t*wd-t1*w1-t1*wd)*wd*exp(-
D*t*w+D*t1*w)*w*w1^2-D*sin(t*wd-t1*w1-t1*wd)*wd^2*exp(-
D*t*w+D*t1*w)*w*w1+4*D*sin(w1*t)*w1^2*w*wd-sin(t*wd+t1*w1-t1*wd)*D*w*exp(-
D*t*w+D*t1*w)*w1^3+cos(t*wd+t1*w1-t1*wd)*wd^2*exp(-D*t*w+D*t1*w)*w1^2-cos(t*wd+t1*w1-
t1*wd)*wd^3*exp(-D*t*w+D*t1*w)*w1-sin(t*wd-t1*w1-t1*wd)*D*w*exp(-D*t*w+D*t1*w)*w1^3-cos(t*wd-
t1*w1-t1*wd)*wd^2*exp(-D*t*w+D*t1*w)*w1^2-cos(t*wd-t1*w1-t1*wd)*wd^3*exp(-D*t*w+D*t1*w)*w1-
D^3*sin(t*wd+t1*w1-t1*wd)*w^3*exp(-D*t*w+D*t1*w)*w1-D^3*sin(t*wd-t1*w1-t1*wd)*w^3*exp(-
D*t*w+D*t1*w)*w1+2*D^2*cos(w1*t)*w1*w^2*wd-D^2*cos(t*wd+t1*w1-t1*wd)*w^2*exp(-
D*t*w+D*t1*w)*w1^2+D^2*cos(t*wd-t1*w1-t1*wd)*w^2*exp(-D*t*w+D*t1*w)*w1^2-D^2*cos(t*wd+t1*w1-
t1*wd)*wd*exp(-D*t*w+D*t1*w)*w^2*w1-2*D^2*cos(t*wd+t1*w1-t1*wd)*wd^2*exp(-D*t*w+D*t1*w)*w^2-
D^2*cos(t*wd-t1*w1-t1*wd)*wd*exp(-D*t*w+D*t1*w)*w^2*w1+2*D^2*cos(t*wd-t1*w1-t1*wd)*wd^2*exp(-
D*t*w+D*t1*w)*w^2-2*D*sin(t*wd+t1*w1-t1*wd)*wd*exp(-D*t*w+D*t1*w)*w*w1^2+2*cos(w1*t)*w1*wd^3-
D^4*cos(t*wd+t1*w1-t1*wd)*w^4*exp(-D*t*w+D*t1*w)+D^4*cos(t*wd-t1*w1-t1*wd)*w^4*exp(-
D*t*w+D*t1*w)+cos(t*wd+t1*w1-t1*wd)*wd*exp(-D*t*w+D*t1*w)*w1^3-cos(t*wd+t1*w1-t1*wd)*wd^4*exp(-
D*t*w+D*t1*w)+cos(t*wd-t1*w1-t1*wd)*wd*exp(-D*t*w+D*t1*w)*w1^3+cos(t*wd-t1*w1-t1*wd)*wd^4*exp(-
D*t*w+D*t1*w)-2*cos(w1*t)*w1^3*wd;

% displacement & velocity
qn2(n)=exp(-D*w*t2)*(AA(n)*cos(wd*t2)+BB(n)*sin(wd*t2)+(Am*Cn(n)*qq)/Bn(n)*wd*qq1);

qndt2(n)=-D*w*exp(-D*w*t2)*(AA(n)*cos(wd*t2)+BB(n)*sin(wd*t2))+exp(-D*w*t2)
*(-1*AA(n)*wd*sin(wd*t2)+BB(n)*wd*cos(wd*t2))+(Am*Cn(n)*qqq)/(Bn(n)*wd*qq1);

   qn1(n)=qn2(n);
   qndt1(n)=qndt2(n);

   for num=1:length(S(:,n))
      Sn(num,n)=S(num,n)*qn2(n); % Deflection of the nth mode
   end

end

 Sfinal=Sn(:,1)+Sn(:,2)+Sn(:,3); % vibration solution w(x,t)

% Get the max lateral displacement of steady state
if abs(Sfinal(376))>MaxDis && t>TS
   MaxDis=abs(Sfinal(376));
end

%============ electric output ============

slopdiff(tn)=(Sfinal(Mark2-1)-Sfinal(Mark2-2))/dx-(Sfinal(Mark1+2)-Sfinal(Mark1+1))/dx;

Q(tn)=-e31*b*(h+h1)/2*slopdiff(tn);
charge=[charge,Q(tn)];
```

```
V(tn)=Q(tn)/Cv;


if V(tn)>43.3
    Stoptune=1;
end

if abs(V(tn))>Vc(tn-1) && Stoptune == 0

  Vc(tn)=Vc(tn-1)*exp(-tx/(R*Cvo))
+exp(-t2/(R*Cvo))*(abs(Voutput(tn-1))*exp(t1/(R*Cvo))
+abs(V(tn))*exp(t2/(R*Cvo)))/(2*R*Cvo)*tx;

  Vfeedback=Vc(tn);
  P=e33*Vfeedback/Ah*0.00018;
  RE=1;

else

  Vc(tn)=Vc(tn-1);
  RE=0;

end

Voutput(tn)=(V(tn)+V(tn-1))/2;


tn=tn+1;

end

SumPe=0;
for i=2:length(charge)

   II(i-1)=(charge(i)-charge(i-1))/tx;
   Pe=2*II(i-1)*Voutput(i+1);
   PE=[PE,Pe];
   SumPe=SumPe+Pe^2*tx;

end

RMSPe=sqrt(SumPe/TD);
```

Appendix B: List of publications in MSc research

Submitted Journal Paper (1):

Y. Cheng, N. Wu and Q. Wang, An efficient piezoelectric energy harvester with self-frequency tuning, *Journal of Sound and Vibration.* (Under review)

Referred Conference Papers (2):

Y. Cheng, N. Wu, and S. Zhao. "Study on High Efficiency Energy Harvesting Using Piezoelectric Coupled Beam With Self-Tuning Process." *ASME 2015 International Mechanical Engineering Congress and Exposition.* American Society of Mechanical Engineers, 2015.

S. Zhao, N. Wu, and Y. Cheng. "High Sensitivity Damage Detection With Vibration Mode Shape Tuning Through the Optimal Design of Piezoelectric Actuators." ASME 2015 International Mechanical Engineering Congress and Exposition. American Society of Mechanical Engineers, 2015.